The origin of Zn isotope fractionation in sulfides

Toshiyuki Fujii, Frédéric Moynier, Marie-Laure Pons, Francis Albarède

Original Paper

The origin of Zn Isotope Fractionation in Sulfides

Toshiyuki Fujii[1]*, Frédéric Moynier[2], Marie-Laure Pons[3], and Francis Albarède [3]

[1] Research Reactor Institute, Kyoto University, 2-1010 Asashiro Nishi, Kumatori, Sennan, Osaka 590-0494, Japan

[2] Department of Earth and Planetary Sciences and McDonnell Center for Space Sciences, Washington University in St. Louis, Campus Box 1169, 1 Brookings Drive, Saint Louis, MO 63130-4862, USA

[3] Ecole Normale Supérieure de Lyon, Université de Lyon 1, CNRS, 46, Allee d'Italie, 69364 Lyon Cedex 7, France

*Author to whom correspondence should be addressed

tosiyuki@rri.kyoto-u.ac.jp

TEL: +81-72-451-2469, FAX: +81-72-451-2634

Abstract:

Isotope fractionation of Zn between aqueous sulfide, chloride, and carbonate species (Zn^{2+}, $Zn(HS)_2$, $Zn(HS)_3^-$, $Zn(HS)_4^{2-}$, $ZnS(HS)^-$, $ZnCl^+$, $ZnCl_2$, $ZnHCO_3^+$, and $ZnCO_3$) was investigated using *ab initio* methods. Only little fractionation is found between the sulfide species, whereas carbonates are up to 1‰ heavier than the parent solution. At pH>3 and under atmospheric-like CO_2 pressures, isotope fractionation of Zn sulfides precipitated from sulfidic solutions is affected by aqueous sulfide species and the $\delta^{66}Zn$ of sulfides reflect these in the parent solutions. Under high P_{CO_2} conditions, carbonate species become abundant. In high P_{CO_2} conditions of hydrothermal solutions, Zn precipitated as sulfides is isotopically nearly unfractionated with respect to a low-pH parent fluid. In contrast, negative $\delta^{66}Zn$ down to at least −0.6‰ can be expected in sulfides precipitated from solutions with pH>9. Zinc isotopes in sulfides and rocks therefore represent a potential indicator of mid to high pH in ancient hydrothermal fluids.

Keywords: Zinc, ligand, ocean, quantum chemical calculation, isotope fractionation

1. INTRODUCTION

Measurements of isotopic variations of Zn with a precision routinely better than 50 ppm have been reported in natural samples (see Albarede, 2004; Cloquet, 2008 for reviews). Presently, the interpretation of these isotopic variations is limited by our knowledge of the fractionation involved during chemical reactions, especially for species relevant to the present and ancient oceans, such as Zn chloride and Zn sulfides. Isotope fractionations created in Zn(II)-Zn(II) ligand exchange reactions (Maréchal and Albarède, 2002; Fujii et al., 2010) and in Zn(II)-Zn^0 redox reactions (Kavner et al., 2008; Fujii et al., 2009a) have been experimentally observed. Preliminary estimates of Zn isotope fractionation were provided in abstract form by Schauble (2003), while extensive calculations using *ab initio* techniques allowed Zn isotope fractionation to be assessed for aquo-, chloro-, sulfato-, and other dissolved Zn^{2+} species (Black et al., 2011).

The role of sulfides is central to a broad range of prevalent geological scenarios and in particular the status of sulfur in ancient oceans is an outstanding issue (Canfield, 1998). Thermodynamic calculations for Zn sulfides and hydrosulfides have been carried out with the aim of assessing the chemistry of Proterozoic and Archean oceans (Saito et al., 2003). Hydrothermal vent solutions discharging either at mid-ocean ridges (Edmond et al., 1979) or along subduction zones (Mottl et al., 2004) comprise another environment dominated by sulfides. The solubility of sphalerite (ZnS) and speciation in sulfide solutions have also been studied (Bourcier and Barnes, 1987; Hayashi et al., 1990; Daskalakis and Helz, 1993; Tagirov et al., 2007; Tagirov and Seward, 2010). Tagirov et al. (2007) determined the stoichiometry and stability of Zn sulfide/hydrosulfide complexes at 373 K and concluded that the major species are

64 $Zn(HS)_2^0$, $Zn(HS)_3^-$, and $ZnS(HS)^-$. Their Zn speciation model was consistent with that
65 of Bourcier and Barnes (1987), but different from other models (Hayashi et al., 1990;
66 Daskalakis and Helz, 1993), and was further expanded and strengthened in recent work
67 (Tagirov and Seward, 2010). The present work takes on the task of evaluating Zn
68 speciation and isotope fractionation among the different Zn sulfide species present in
69 geological fluids between 298 and 573 K. It largely relies on the stability analysis of
70 Tagirov et al. (2010) and complements the recent work by Black et al. (2011) on Zn
71 isotope fractionation in solution.
72
73 **2. COMPUTATIONAL METHODS**
74 Orbital geometries and vibrational frequencies of aqueous Zn(II) species were computed
75 using density functional theory (DFT) as implemented by the Gaussian03 code (Frisch
76 et al., 2003). The DFT method employed here is a hybrid density functional consisting
77 of Becke's three-parameter non-local hybrid exchange potential (B3) (Becke, 1993)
78 with Lee-Yang and Parr (LYP) (Lee et al., 1988) non-local functionals. In a quantum
79 chemical study, the convergence of the reaction energies of Zn(II) species is excellent in
80 6-311+G(d,p) or higher basis sets (Rulíšek and Havlas, 1999). Hence, the 6-311+G(d,p)
81 basis set, which is an all-electron basis set, was chosen for H, C, O, S, and Zn. For the
82 solvation effect, the CPCM continuum solvation method (CPCM: conductor-like
83 polarizable continuum model) was used. The geometry optimization and intramolecular
84 vibrational frequency analysis were performed for the hydrated Zn ion, hydrated Zn
85 carbonates, and hydrated Zn sulfides. For hydrated Zn chlorides, the results were
86 reproduced from our previous study (Fujii et al., 2010).
87

3. RESULTS AND DISCUSSION

3.1 Basis for the isotope fractionation theory in systems at equilibrium

A chemical exchange reaction can be represented as two half-reactions,

$$AX + Y \rightleftarrows AY + X, \quad (1)$$

or

$$A'X + Y \rightleftarrows A'Y + X, \quad (2)$$

where A and A' are the heavy and light isotopes of the element A, and X and Y represent ligands. The difference between half-reactions 1 and 2 corresponds to an isotopic exchange reaction between AX and AY,

$$A'Y + AX \rightleftarrows A'X + AY, \quad (3)$$

The isotope separation factor α between AX and AY is defined as

$$\alpha = \frac{([A]/[A'])_Y}{([A]/[A'])_X} \quad (4)$$

where $([A]/[A'])_X$ and $([A]/[A'])_Y$ are the isotopic ratios of A/A' measured in the complexes AX (and A'X) and AY (and A'Y), respectively. The isotope enrichment factor is defined as $\alpha_m - 1$. Since α is close to 1, $\alpha - 1$ can be approximated as $\ln \alpha$.

105 Isotopic deviations in parts per 1000 are conventionally defined as

$$\delta = \left(\frac{([A]/[A'])_{species}}{([A]/[A'])_{reference}} - 1 \right) \times 1000 \quad (5)$$

106

107 If AX (and A'X) is the major component in the system, $\Sigma[A]/\Sigma[A']$ is approximated to
108 be $([A]/[A'])_X$ such that an approximation expression $\delta \approx 10^3 \ln \alpha$ works.

109 The standard theory of chemical isotope fractionation is based on
110 mass-dependent isotopic differences in vibrational energies of isotopologues (Urey,
111 1947; Bigeleisen and Mayer, 1947). The isotope enrichment factor is proportional to
112 $\left(\frac{1}{m'} - \frac{1}{m}\right)$ with m and m' the masses of two isotopes (prime represents the light
113 isotope). In a previous study on Zn isotope fractionation, we showed that the
114 contribution of other effects, such as the nuclear field shift effect (Bigeleisen, 1996;
115 Nomura et al., 1996; Fujii et al., 2009b) to $\ln \alpha$ is <10% (Fujii et al., 2010). Therefore,
116 an adequate approximation of fractionation factors between different species may be
117 obtained by the conventional mass-dependent theory (Bigeleisen and Mayer, 1947). All
118 the calculations were made for the $^{66}Zn/^{64}Zn$ ratio which avoids odd even staggering
119 (King, 1984; Aufmuth et al., 1987; Fricke and Heilig, 2004; Fujii et al., 2009b).

120 The isotope enrichment ($\ln \alpha$) due to the intramolecular vibrations can be
121 evaluated from the reduced partition function ratio (RPFR) $(s/s')f$ (Bigeleisen and Mayer,
122 1947; Urey, 1947) defined as

123

$$\ln (s/s')f = \Sigma[\ln b(u_i') - \ln b(u_i)] \quad (6)$$

124 where

$$\ln b(u_i) = -\ln u_i + u_i/2 + \ln (1 - e^{-ui}) \quad (7)$$

In this equation, ν stands for vibrational frequency, *s* for the symmetry number of the molecule, and $u_i = h\nu_i/kT$. The subscript *i* stands for the *i*th molecular vibrational level with primed variables referring to the light isotopologue. The isotope enrichment factor due to the molecular vibration can be evaluated from the frequencies summed over all the different modes. The partition function ratio (*s*/*s*')*f* for isotopologues A'X and AX (A'Y and AY, respectively) is noted β_X (β_Y, respectively). In the isotopic exchange reaction 3, isotope fractionation can be estimated from the relation $\ln \alpha \approx \ln \beta_Y - \ln \beta_X$.

In the present study, the optimized structures of hydrated Zn^{2+} and hydrated Zn sulfides were first analyzed for ^{64}Zn. For each complex, intramolecular vibrational frequencies (ν_i) were analyzed. By substituting ν_i into Eq. (7), $\ln b(u_i')$ was determined. Using the same molecular structures, ^{64}Zn was replaced by ^{66}Zn and the vibrational frequency analysis was performed again to obtain $\ln b(u_i)$, from which ln β was then determined.

3.2. Assessment of *ab initio* calculations

The isotope fractionation between hydrated Zn^{2+} and aqueous Zn chlorides has been investigated experimentally and theoretically at 294 K (Fujii et al., 2010). Calculations carried out for $Zn(H_2O)_6^{2+}$, $Zn(H_2O)_{18}^{2+}$, $ZnCl(H_2O)_5^{+}$, $ZnCl_2(H_2O)_4$, $ZnCl_3(H_2O)_3^{-}$, $ZnCl_3(H_2O)^{-}$, $ZnCl_4(H_2O)_2^{2-}$, and $ZnCl_4^{2-}$, allow for a comparison with the work of Black et al. (2011). As intramolecular vibrational modes and their frequencies depend on the cluster model and interatomic distances, the stability of each compound must first be demonstrated. We first tested the effect of solvation of Zn^{2+} ions by comparing

148 the small cluster $Zn(H_2O)_6^{2+}$, including only the first hydration shell (Fig. 1a and
149 electronic annex, Fig. S1) with the large cluster $Zn(H_2O)_{18}^{2+}$, in which the small cluster
150 is surrounded by 12 H_2O molecules in a second hydration shell (see figure 1b of Li et al.,
151 1996). In the present study, the CPCM continuum solvation method was tested. For
152 $Zn(H_2O)_6^{2+}$, we used the dielectric constant of water $\varepsilon = 78.3553$. The results are shown
153 in Table 1 and were found to be consistent with those of Fig. 9 in Black et al. (2011)
154 (see electronic annex, Tables S1, S2, and S3). The presence of the second hydration
155 shell shortens the Zn-O bond distance by 0.014 Å in the first coordination shell.
156 Applying the CPCM method further shortens this distance by 0.012 Å. The CPCM
157 solvation method provides bond distances satisfactorily close to those obtained
158 experimentally (Dreier and Rabe, 1986; Matsubara and Waseda, 1989; Maeda et al.,
159 1995).

160 The calculated ν_1 frequencies (totally symmetric vibration, see Fig. S1) of
161 $Zn(H_2O)_6^{2+}$ in this study and Fujii et al. (2010) are much smaller than the literature
162 values obtained experimentally (Table 1). With the second hydration shell present, the
163 calculated ν_1 frequency of $Zn(H_2O)_{18}^{2+}$ agrees with the experimental value of 380 cm^{-1}
164 (Yamaguchi et al., 1989). This frequency was not reproduced very well when the
165 CPCM method was applied to a model including only the inner hydration shell.

166 Since the conventional Bigeleisen-Mayer equation (Bigeleisen and Mayer,
167 1947) involves vibrational frequencies, an accurate evaluation of ν_1 is in order. Besides
168 ν_1, other vibrational modes, *e.g.*, asymmetric modes of ν_3 and so on (see Fig. S1), are
169 also important to evaluate RPFR (see Eqs. 6 and 7 and Black et al., 2011). The ν_2 and ν_3
170 frequencies are shown in Table 1. As for ν_1, adding the second hydration shell increases
171 the ν_2 and ν_3 frequencies and brings them closer to experimental observations (Rudolph

and Pye, 1999; Mink et al., 2003). Addition of the second hydration shell is therefore more effective than resorting to the CPCM solvation method.

The ln β values at 273, 423, and 573K (25, 150, and 300°C, respectively) calculated by using Eqs. (6) and (7) are shown in Table 2. The accuracy in RPFRs estimated by *ab initio* method is discussed in Rustad et al. (2010). It is clear that applying the CPCM solvation method does not significantly affect the value of ln β, whereas adding a second hydration shell with 12 H_2O molecules increases ln β by 0.3‰ at 298 K. A similar phenomenon was found in our previous study on Pd^{2+} isotope fractionation (Fujii et al., in press).

3.3. β-factors of aqueous Zn sulfides

The structure of the Zn sulfides was calculated with small cluster models without additional shells. Zn^{2+} and Zn hydrogensulfides are related through the following stepwise reactions,

$$Zn^{2+} + HS^- \rightleftarrows ZnSH^+ \quad (8)$$

$$ZnHS^+ + HS^- \rightleftarrows Zn(HS)_2 \quad (9)$$

$$Zn(HS)_2 + HS^- \rightleftarrows Zn(HS)_3^- \quad (10)$$

$$Zn(HS)_3^- + HS^- \rightleftarrows Zn(HS)_4^{2-} \quad (11)$$

190

191 *Calculations for $ZnSH^+$.*

192 The formation of Zn mono-hydrogensulfide has been suggested on the basis of
193 voltammetric data (Zhang and Millero, 1994), but was later questioned (Luther et al.,
194 1996). Reaction 8 was disregarded by studies on sphalerite (ZnS) solubility in sulfide
195 solutions (Bourcier and Barnes, 1987; Hayashi et al., 1990; Daskalakis and Helz, 1993;
196 Tagirov et al., 2007; Tagirov and Seward, 2010). Though we tested the structural
197 optimization of $ZnHS(H_2O)_5^+$, this model complex is unstable and deforms into
198 $ZnHS(H_2O)_4^+$ with the 5th water molecule moving out of the inner coordination shell,
199 which suggests that the stability constant of reaction 8 is very small. A
200 hydroxide-hydrogensulfide species, $Zn(OH)HS^+$, has been reported (Bourcier and
201 Barnes, 1987; Hayashi et al., 1990), but its existence was not confirmed (Tagirov et al.,
202 2007; Tagirov and Seward, 2010).

203

204 *Calculations for $Zn(HS)_2$.*

205 In a theoretical study on Zn sulfides (Tossell and Vaughan, 1993), a tetrahedral
206 structure $Zn(HS)_2(H_2O)_2$ has been reported as $Zn(HS)_2$. The structure of
207 bis-hydrogensulfide for six-coordination transition metals is considered to be similar to
208 that of *trans*-$Mn(HS)_2(H_2O)_4$ (Rickard and Luther, 2006). We calculated the optimized
209 structure for the recommended structure $Zn(HS)_2(H_2O)_4$ (Fig. 1b) and the bond lengths
210 are shown in Table 1. The ln β value at 298 K is 2.72‰.

211

Calculations for $Zn(HS)_3^-$.

The calculations for the 6-coordinated $Zn(HS)_3(H_2O)_3^-$ did not converge. HS^- forms stronger bonds with Zn^{2+} than H_2O, and 3 HS^- molecules tend to form a triangle, with Zn^{2+} at the center (see figure 1 of Tossell and Vaughan, 1993). Tossell and Vaughan (1993) reported that $Zn(HS)_3^-$ and $Zn(HS)_3(OH)^{2-}$ are the most stable of the tri-hydrogensulfide species. The hydrolyzed species $Zn(HS)_3(OH)^{2-}$ has been considered in earlier solubility studies of sphalerites (Hayashi et al., 1990; Daskalakis et al., 1993), but its existence was later dismissed (Tagirov et al., 2007; Tagirov and Seward, 2010).

The existence of a species $Zn(HS)_3^-$ lacking direct Zn-water coordination is unlikely in aqueous solution. Tossell and Vaughan (1993) reported the presence of the mono-hydrated tri-hydrogensulfide species, $Zn(HS)_3H_2O^-$, and our calculations reproduced this structure (see figure 1 of Tossell and Vaughan, 1993). $Zn(HS)_3$ keeps the triangular plane with one H_2O molecule bound to the plane via a hydration bond (H_2O-Zn^{2+}) and OH_2-SH hydrogen bonds. The hydrogen bond appears stronger than the hydration bond, which suggests that an extra H_2O molecule may bind to the opposite side of the $Zn(HS)_3$ plane to form $Zn(HS)_3(H_2O)_2^-$. The structure after convergence is shown in Fig. 1c. However, even though the plane symmetric arrangement with two H_2O molecules with respect to the $Zn(HS)_3$ plane is possible, the Gibbs free energy was 1.09 kJ/mol larger and this model complex is therefore not chosen.

The bond distances are shown in Table 3. The longer Zn-O bond distance suggests that the H_2O molecules possibly are bound to $Zn(HS)_3$ via the hydrogen bonds of OH_2-SH. The ln β value at 298 K is 3.03‰ (Table 2).

235

236 *Calculations for $Zn(HS)_4^{2-}$.*

237 Solubility measurements of sphalerites in sulfide solutions (Bourcier and Barnes, 1987;
238 Hayashi et al., 1990; Daskalakis and Helz, 1993) considered the presence of a
239 tetra-hydrogensulfide species $Zn(HS)_4^{2-}$; its mole fraction is expected to decrease with
240 temperature (Tagirov and Seward, 2010). A possible tetrahedral structure (Fig. 1d) was
241 suggested by Tossell and Vaughan (1993). The tetrahedral structure of $Zn(HS)_4^{2-}$ is
242 similar to a unit cell of Zn sulfide clusters (Luther et al., 1999; Luther and Rickard,
243 2005). Our results are shown in Tables 2 and 3. The ln β value at 298 K shows the
244 smallest value (2.19‰, Table 2) of all Zn sulfides.

245

246 *Calculations for $ZnS(HS)^-$.*

247 A distinctive feature in the solubility trend of sphalerite calculated by Tagirov et al.
248 (2007) and Tagirov and Seward (2010) is that $ZnS(HS)^-$ appears to be a prevalent
249 sulfide species at pH>10 and temperatures <473 K. With increasing pH, complexation
250 proceeds from $Zn(HS)_3^-$ to $Zn(HS)_4^{2-}$ and $ZnS(HS)^-$ (Tagirov and Seward, 2010).
251 Formation of $ZnS(HS)^-$ from $Zn(HS)_4^{2-}$ with increasing pH results from the reaction

252

$$Zn(HS)_4^{2-} + OH^- \rightleftarrows ZnS(HS)(H_2O)^- + 2HS^- \quad (12)$$

253

254 A few *ab initio* calculation studies on anhydrous Zn sulfides (Cini, 1999) or clusters of
255 Zn sulfides (Luther et al., 1999; Luther and Rickard, 2005) have been reported. To the
256 best of our knowledge, structural data of monomeric $ZnS(HS)^-$ in aqueous solutions are

not available. Spatially, water molecules may interact with Zn(II) in $ZnS(HS)^-$ as $ZnS(HS)(H_2O)_n^-$. The coordination number of Zn(II) in the monomeric species $ZnS(HS)(H_2O)^-$ is three, but this coordination number is too small if this species exists in aqueous solution. Since the aggregation of complexes increases the coordination probability, $ZnS(HS)(H_2O)^-$ is considered to be a simplified formula of polymerized species $n[ZnS(HS)(H_2O)^-]$. Let us consider a dimer for $n = 2$.

Stereochemically, dimerization of $ZnS(HS)^-$ from $Zn(HS)_3(H_2O)_3^-$ may be natural (see Fig. 1c and 1e).

$$2Zn(HS)_3(H_2O)_2^- + 2OH^- \rightleftarrows Zn_2S_2(HS)_2(H_2O)_2^{2-} + 2SH^- + 4H_2O \quad (13)$$

where $Zn_2S_2(HS)_2(H_2O)_2^{2-}$ can be expressed as $2[ZnS(HS)H_2O^-]$. Zn(II) has a coordination number of 5 in this species. Since S^{2-} has the tetrahedral coordination property, two S^{2-} ions bridging to two Zn^{2+} ions may also bind to H_2O in the outer sphere. More H_2O molecules may be arranged on the triangular $Zn(HS)_3$ plane. $ZnS(HS)(H_2O)_n^-$ with $n \geq 2$ may exist.

$Zn(HS)_3^-$ and $ZnS(HS)^-$ possess the trigonal planar of ZnS_3 core, while $Zn(HS)_4^{2-}$ is tetrahedral. Large entropic changes via structural changes in the reaction $Zn(HS)_3^- \leftrightarrow Zn(HS)_4^{2-} \leftrightarrow ZnS(HS)^-$ are expected due to the existence of intermediate state $Zn(HS)_4^{2-}$. With the increase of temperature, the mole fraction of $Zn(HS)_4^{2-}$ drastically decreases (Tagirov and Seward, 2010). This suggests a direct reaction pathway between $Zn(HS)_3^-$ and $ZnS(HS)^-$ at high temperatures. This reaction path of

278 reaction 13 would be entropically favorable. The bond distances of 2[$ZnS(HS)H_2O^-$] are
279 shown in Table 3. The ln β value at 298 K is 2.63‰ (Table 2).
280
281 *Calculations for Zn carbonates.*
282 In the present work, we calculated the ln β values for Zn isotope fractionation
283 (Table 2) for hydrated Zn carbonates, $ZnHCO_3(H_2O)_4$, and $ZnCO_3(H_2O)_4$, in which
284 HCO_3^- and CO_3^{2-} are treated as bidentate ligands (see Figs. 1f and 1g) using the same
285 techniques as Fujii et al. (2011) for Ni. Zinc is isotopically heavy in carbonates relative
286 to hydrated Zn^{2+} and Zn sulfide species. The ln β values are larger than those of
287 $Zn(H_2O)_6^{2+}$, Zn sulfides, and Zn chlorides. They compare with the ln β values reported
288 by Black et al. (2011) on Zn sulfates. Upon reduction of sulfates to sulfides in the
289 presence of carbonate ions, a strong fractionation of Zn isotopes may be expected in the
290 sulfide-carbonate system.
291
292 **3.4. Zn isotope systematics between aqueous sulfides and chlorides**
293 Isotope fractionation relevant to $Zn(H_2O)_6^{2+}$, $Zn(HS)_2(H_2O)_4$, $Zn(HS)_3(H_2O)_2^-$,
294 $Zn(HS)_4^{2-}$, 2[$ZnS(HS)H_2O^-$], $ZnCl(H_2O)_5^+$, $ZnCl_2(H_2O)_4$, $ZnHCO_3(H_2O)_4^+$, and
295 $ZnCO_3(H_2O)_4$ will now be evaluated. The structure and ln β of Zn chlorides were
296 reproduced from our previous study (Fujii et al., 2010) with calculations extended to
297 higher temperatures. The temperature dependence of ln β can be estimated from the
298 values compiled in Table 2. The total range of variation of ln β at 298 K is ~2‰. We
299 calculated the speciation and isotopic fractionation of Zn for a total concentration of
300 sulfur Σ[S] of 0.1 M in the absence of Cl^- ([Cl^-] = 0 M) and carbonates (Σ[C] = 0 M) at

298, 423, and 573 K as a function of pH. In our calculation, free Cl^- concentration is just treated as a parameter without considering association/dissociation reactions of HCl and chlorides at various temperatures. In principle, activities should be used throughout rather than concentrations, but the precise compositions of hydrothermal solutions are rarely known, and uncertainties on isotope fractionation attached to the non-ideal character of electrolyte solutions are certainly negligible with respect to those resulting from the poorly constrained chemistry of hydrothermal systems. As a result, the activity coefficients were considered equal to unity. As a dilute system, molar concentrations are used instead of molal concentrations. All calculations were performed under an assumption that the molecular structures remain the same by increasing temperature.

The following chemical equilibrium reactions were investigated,

$$Zn^{2+} + 2HS^- \rightleftarrows Zn(HS)_2, \quad K_{Zn(HS)_2} \tag{14}$$

$$Zn^{2+} + 3HS^- \rightleftarrows Zn(HS)_3^-, \quad K_{Zn(HS)_3^-} \tag{15}$$

$$Zn^{2+} + 4HS^- \rightleftarrows Zn(HS)_4^{2-}, \quad K_{Zn(HS)_4^{2-}} \tag{16}$$

$$Zn^{2+} + 2HS^- \rightleftarrows ZnS(HS)^- + H^+, \quad K_{ZnS(HS)^-} \tag{17}$$

317 It should be noted that, in the present study, we use *K* for cumulative formation constant
318 β in order to avoid confusion about ln β of isotope fractionation.
319 Under reducing conditions with negligible sulfate formation, the total concentration of
320 sulfur (Σ[S] = 0.1 M) is controlled by the following dissociation reaction,
321

$$H_2S \rightleftarrows HS^- + H^+ \tag{18}$$

322
323 where we used the relation,

$$\log \frac{[HS^-]}{[H_2S]} = -pK_a + pH \tag{19}$$

324
325 The stability constants and acid dissociation constants (pK_a) at 298, 423, and 573 K
326 used are listed in Table 4. Since pK_a was determined under the existence of Na^+, strictly,
327 it includes an effect of NaHS dissociation.
328 We also calculated the speciation and isotopic fractionation of Zn isotologues
329 under typical hydrothermal conditions, with Σ[S] = 5 mM (Von Damm, 1990) and $[Cl^-]$
330 = 0.55 M (Macleod et al., 1994) at 298, 423, and 573 K and for variable pH. We set
331 P_{CO_2} at 50 bar ($\log P_{CO_2} = 1.6$), which corresponds to a water (total) pressure of 10^5
332 Pa (1 kbar) and a mole fraction of CO_2 of 5 percent (Rose et al., 1996). Such values
333 conveniently describe the conditions at about 3 km below the sea floor. The following
334 chemical equilibrium reactions also were investigated,
335

$$Zn^{2+} + Cl^{-} \rightleftarrows ZnCl^{+}, \quad K_{ZnCl^{+}} \tag{20}$$

336

$$Zn^{2+} + 2Cl^{-} \rightleftarrows ZnCl_2, \quad K_{ZnCl_2} \tag{21}$$

337

$$Zn^{2+} + HCO_3^{-} \rightleftarrows ZnHCO_3^{+}, \quad K_{ZnHCO_3^{+}} \tag{22}$$

338

$$Zn^{2+} + CO_3^{2-} \rightleftarrows ZnCO_3, \quad K_{ZnCO_3} \tag{23}$$

339

340 For carbonates, the following gas-liquid equilibrium reactions were considered.

341

$$CO_2 + H_2O \rightleftarrows HCO_3^{-} + H^{+}, \quad K_{HCO_3^{-}} \tag{24}$$

342

$$CO_2 + H_2O \rightleftarrows CO_3^{2-} + 2H^{+}, \quad K_{CO_3^{2-}} \tag{25}$$

343

344 The ionization of carbonic acid at elevated temperatures has been studied by Read
345 (1975) and Patterson et al. (1982, 1984). The acid dissociation constant between the
346 hydrogen carbonate ion (HCO_3^{-}) and the carbonate ion (CO_3^{2-}) is the ratio of $K_{HCO_3^{-}}$
347 and $K_{CO_3^{2-}}$. These values at 298, 423, and 573 K (Smith et al., 1986), in which the
348 original data are taken from (Patterson et al., 1982; 1984), are shown in Table 4.

Because of the broad relevance of carbon dioxide to geological environments, we first investigated the effect of P_{CO_2} on Zn isotope variability of Zn in sulfidic hydrothermal environments. As a reference, speciation and isotope fractionation are first investigated for hydrothermal solutions placed under the low P_{CO_2} typical of equilibration with the modern atmosphere. Then, the discussion is extended to conditions of high P_{CO_2} in order to constrain Zn isotope fractionation in solutions equilibrated with a high-P_{CO_2} atmosphere or circulating in deep-seated hydrothermal systems.

The results are shown in Figs. 3, 4, and 5. Figs 3a, 4a, and 5a show quite good agreement with the reported mole fractions of aqueous Zn sulfide species estimated from stability constants of reactions 14-17 and solubility products of ZnS(crystal) (Tagirov and Seward, 2010). In the present study, $K_{ZnHCO_3^+}$ and K_{ZnCO_3} at the standard temperature 298 K (Zirino and Yamamoto, 1972) were used for 423 and 573 K due to lack of reliable data of aqueous Zn carbonates at high temperature. Even if a tenfold larger $K_{ZnHCO_3^+}$ were used for 573 K (Fig 5b), the mole fraction of $ZnHCO_3^+$ would not visibly increase. Variations of K_{ZnCO_3} mainly changes the mole fractions of $ZnCO_3$ and $ZnS(HS)^-$ but have little effect on the concentrations of other species. Increasing log K_{ZnCO_3} by one unit increases the mole fraction of $ZnCO_3$ and decreases that of $ZnS(HS)^-$ by ~25% (see electronic annex, Fig. S2).

Isotope fractionation of Zn observed as $\delta^{66}Zn$ was estimated as shown in Figs. 3c, 3d, 4c, 4d, 5c, and 5d. The $\delta^{66}Zn$ value was calculated as follows. The bulk $^{66}Zn/^{64}Zn$ ratio is

371

$$\frac{\Sigma[^{66}Zn]}{\Sigma[^{64}Zn]} = \frac{\begin{array}{c}[^{66}Zn^{2+}] + [^{66}Zn(HS)_2] + [^{66}Zn(HS)_3^-] + [^{66}Zn(HS)_4^{2-}] + [^{66}ZnS(HS)^-] + [^{66}ZnCl^+] + \\ [^{66}ZnCl_2] + [^{66}ZnHCO_3^+] + [^{66}ZnCO_3]\end{array}}{\begin{array}{c}[^{64}Zn^{2+}] + [^{64}Zn(HS)_2] + [^{64}Zn(HS)_3^-] + [^{64}Zn(HS)_4^{2-}] + [^{64}ZnS(HS)^-] + [^{64}ZnCl^+] + [^{64}ZnCl_2] \\ [^{64}ZnHCO_3^+] + [^{64}ZnCO_3]\end{array}} \quad (26)$$

372

373 Stability constants were calculated from ln β values. For example,

374

$$\ln \frac{K_{Zn(HS)_2}(^{66}Zn)}{K_{Zn(HS)_2}(^{64}Zn)} = \ln \frac{[^{66}Zn(HS)_2]/[^{64}Zn(HS)_2]}{[^{66}Zn^{2+}]/[^{64}Zn^{2+}]}$$

375

$$= \ln \beta_{Zn(HS)_2} - \ln \beta_{Zn^{2+}} \quad (27)$$

376

377 The value $\Sigma[Zn] = 10^{-6.1}$ M (Tagirov and Seward, 2010) was used, but is
378 inconsequential for the speciation calculation. The effect of ionic strength was neglected
379 and activity coefficients of all species were set to be unity in a diluted system, which
380 would be of no practical importance for isotope ratios.

381

382 **3.5 Zn isotope variability in solutions at low to intermediate temperatures**

383 *Low P_{CO_2} conditions.*

384 Isotope fractionation between natural fluids and precipitates occurs when Zn distributes
385 itself between sphalerite, the prevalent Zn ore, and the parent fluid. Figures 3-5 indicate
386 that, as expected from the order of ln β (Figure 2), the various aqueous Zn sulfide
387 complexes are all isotopically lighter than Zn^{2+} and Zn chlorides. Zinc isotope
388 fractionation in sulfide-rich solutions is controlled by the respective mole fractions of
389 hydrated Zn^{2+} and aqueous sulfides and therefore is predicted to be pH-dependent. At

390 pH<3, Zn is largely present as Zn^{2+} in fresh water and as Zn chlorides at seawater
391 chlorinities. High chlorine contents change the charge balance and therefore shift the
392 dependence of speciation with pH, but, overall, affect isotope fractionation patterns only
393 slightly (see electronic, Figs. S3, S4, and S5). Under conditions typical of equilibration
394 with the atmosphere, carbonate complexes can safely be neglected (Zirino and
395 Yamamoto, 1972). Sulfides precipitating from hydrothermal solutions should be
396 isotopically lighter than the solution, but the extent of isotope fractionation decreases
397 with temperature. Zn isotope fractionation between the plausible precursor species of
398 sphalerite, $Zn(HS)_2$ at low pH and $Zn(HS)_4^{2-}$ and/or $ZnS(HS)^-$ at high pH, is very small.
399 At pH>3, the dominant Zn species are aqueous sulfides (Tagirov and Seward, 2010).
400 Under the assumption that the isotopic composition of sphalerite is inherited from the
401 precursor species, little isotope fractionation between sphalerite and the fluid is
402 therefore expected (< 0.25‰) at 423 K and even less at higher temperatures.
403 In sulfide-free oxic seawater and fresh water equilibrated with the atmosphere,
404 metallic ion, chloride, hydroxide, and carbonate complexes dominate zinc speciation,
405 while Zn sulfate is a minor species (Zirino and Yamamoto, 1972; Turner et al., 1981;
406 Stanley and Byrne, 1990; Black et al., 2011). Zn in marine carbonates is about 1‰
407 heavier (Pichat et al., 2003) than seawater ($\delta^{66}Zn$~0‰) (Bermin et al., 2006), which is
408 consistent with Zn isotope fractionation observed at ~298 K between aqueous carbonate
409 species and the metallic ion or its chloride (see electronic annex, Fig. S6). Zn-O bonds,
410 as in zincite (ZnO) (Schauble et al. 2003), zinc sulfates (Black et al., 2011), and
411 presumably other oxo-anions tend to concentrate heavy Zn. An enrichment of Zn heavy
412 isotopes is therefore expected for zinc carbonates. Here we further assume that Zn

isotope fractionation between solid carbonates and the dissolved species $ZnCO_3$ can be neglected.

High P_{CO_2} conditions.

Carbonate, which is usually a minor species in surface waters, becomes a major player in hydrothermal solutions when P_{CO_2} rises at depth. Figs. 3b, 3d, 4b, 4d, 5b, and 5d show that the presence of carbonate ions brings about a stark contrast between regions of low pH (<8) and high pH (>9). We will restrict the discussion to sphalerite precipitation when smithsonite ($ZnCO_3$) does not reach saturation. At low pH (pH < $pK_{HCO_3^-}$), the abundance of the aqueous $ZnCO_3$ species is very low and sphalerite precipitates with nearly the same $\delta^{66}Zn$ as the original fluid, *i.e.*, with very little fractionation. In contrast, at pH>9, most Zn is in aqueous carbonate form. ZnS is considered to be formed from major sulfides $ZnS(HS)^-$ and/or $Zn(HS)_4^{2-}$ via polymerization and dehydration. If isotope fractionation upon precipitation can be neglected, the values of $\delta^{66}Zn$ for $ZnS(HS)^-$ and $Zn(HS)_4^{2-}$ are representative of those eventually found in ZnS. Sphalerite is therefore expected to possess negative $\delta^{66}Zn$ values. Zinc is isotopically more negative in sphalerite with respect to the fluid, by ~1.5‰ at 298 K, ~0.8‰ at 423 K, and ~0.4‰ at 573 K (see $\delta^{66}Zn$ of $ZnS(HS)^-$ and/or $Zn(HS)_4^{2-}$ at pH >9). Strongly negative $\delta^{66}Zn$ in sphalerite therefore represents a potential indicator of high pH in low- to high-temperature hydrothermal fluids.

The narrow range of Zn isotope fractionation, mostly 0.0 to 0.6‰ in natural sphalerite from continental environments (Albarede, 2004; Kelley et al., 2009) and in most serpentines (Pons et al., 2010), together with the lack of strong isotope

435 fractionation between ZnS and hydrothermal vent fluid from mid-ocean ridges at
436 temperatures >523 K (John et al., 2008) can be explained by the predominance of
437 chloride complexes and aquated Zn^{2+} ion in solutions at pH<7. These observations
438 concur with limited computational evidence that sphalerite is not fractionated with
439 respect to tetrahedral $[ZnCl_4]^{2-}$ (Schauble et al., 2003). Sphalerite precipitation therefore
440 seems to take place by disproportionation of an aqueous sulfide species, most likely
441 $Zn(HS)_2(H_2O)_4$ and $ZnS(HS)H_2O^-$. Occasionally high $\delta^{66}Zn$ in hydrothermal fluids
442 (John et al., 2008) may reflect the prevalence of Zn leached out of carbonate and
443 FeMn-hydroxides ($\delta^{66}Zn$ >0.6 ‰) (Maréchal et al., 2000; Pichat et al., 2003) and not
444 from a basaltic source ($\delta^{66}Zn$ ~0.3 ‰).

445 In contrast, the negative $\delta^{66}Zn$ observed by Pons et al. (2010) in the mud
446 serpentine volcanoes of the Mariana associated with high-pH (10-12) interstitial fluids
447 (down to –0.2‰) (Mottl et al. 2004; Hulme et al., 2010), and by Mason et al. (2005) in
448 island arc-type base-metal deposits from the Urals (down to –0.4 ‰) carry the signature
449 of fractionation by sulfides in island arc hydrothermal solutions dominated by sulfate
450 and carbonates. Zinc-sulfate complexes are weak and much less abundant than chloride
451 and hydroxide complexes, even with the rather high sulfate contents typical of seawater
452 (Stanley and Byrne, 1990; Mottl et al. 2004; Black et al., 2011). The negative $\delta^{66}Zn$
453 values of sulfides precipitated from hydrothermal fluids therefore signal the stability of
454 Zn carbonates and hence pH in excess of the second pK_a of carbonic acid. Zinc isotope
455 compositions in sulfides and rocks are potentially helpful in distinguishing low-pH from
456 high-pH hydrothermal solution.
457

CONCLUSIONS

Isotope fractionation of Zn in aqueous sulfidic solutions was found to be controlled by aqueous zinc sulfide species, and for high P_{CO_2} conditions, by zinc carbonate species. In solutions equilibrated with the atmosphere, Zn is isotopically unfractionated in sulfides and isotopically heavy in carbonates. Under the high P_{CO_2} conditions of hydrothermal solutions, Zn precipitated as sulfides is isotopically nearly unfractionated with respect to a low-pH parent fluid. Negative δ^{66}Zn down to 0.6‰ can be expected in sulfides precipitated from solutions with high P_{CO_2} and a pH > 9. Zn isotopes in sulfides and rocks therefore represent a potential indicator of mid to high pH in ancient hydrothermal fluids.

ACKNOWLEDGMENTS

The authors thank the anonymous reviewers for their useful suggestions, and are grateful to Associate Editor Edwin Schauble, for catching a major problem in an early version of this manuscript and for constructive comments on the manuscript. The authors thank Janne Blichert-Toft for help in improving the English.

476 **REFERENCES**

477 Albarède, F. (2004) The stable isotope geochemistry of copper and zinc. *Rev. Mineral.*
478 *Geohem*. **55**, 409-427.

479 Aufmuth P., Heilig K. and Steudel A. (1987) Changes in mean-square charge radii from
480 optical isotope shifts. *Atom. Data Nucl. Data Tables* **37**, 455-490.

481 Becke A. D. (1993) Density-functional thermochemistry. 3. The role of exact exchange.
482 *J. Chem. Phys*. **98**, 5648-5652.

483 Bermin J., Vance D., Archer C., and Statham P. J. (2006) The determination of the
484 isotopic composition of Cu and Zn in seawater. *Chem. Geol*., **226**, 280-297.

485 Bigeleisen J. and Mayer M. G. (1947) Calculation of equilibrium constants for isotopic
486 exchange reactions. *J. Chem. Phys*. **15**, 261-267.

487 Bigeleisen J. (1996) Nuclear size and shape effects in chemical reactions. isotope
488 chemistry of the heavy elements. *J. Am. Chem. Soc*. **118**, 3676-3680.

489 Black J. R., Kavner A., and Schauble E. A. (2011) Calculation of equilibrium stable
490 isotope partition function ratios for aqueous zinc complexes and metallic zinc.
491 *Geochim. Cosmochim Acta*, **75**, 769-783.

492 Bourcier W. L. and Barnes, H. L. (1987) Ore solution chemistry VII. Stabilities of
493 chloride and bisulfide complexes of zinc to 350°C. *Economic Geol*. **82**, 1839-1863.

494 Canfield D. E., (1998) A new model for Proterozoic ocean chemistry. *Nature* **396**,
495 450-453.

496 Cini R. (1999) Molecular orbital study of complexes of zinc(II) with sulphide,
497 thiomethanolate, thiomethanol, dimethylthioether, thiophenolate, formiate, acetate,
498 carbonate, hydrogen carbonate, iminomethane and imidazole. Relationships with

499 structural and catalytic zinc in some metallo-enzymes. J. Biomol. Struct. Dynamics
500 16, 1225-1237.
501 Cloquet C., Carignan J., Lehmann, M. F., and Vanhaecke F. (2008) Variation in the
502 isotopic composition of zinc in the natural environment and the use of zinc isotopes
503 in biogeosciences: a review. *Anal. Bioanal. Chem*., **390**, 451-463.
504 Daskalakis K. and Helz G. R. (1993) The solubility of sphalerite (ZnS) in sulfidic
505 solutions at 25°C and 1 atm pressure. *Geochim. Cosmochim. Acta* **57**, 4923-4931.
506 Dreier P. and Rabe P. (1986) EXAFS -study of the Zn^{2+} coordination in aqueous halide
507 solutions. *J. Phys. Paris Colloq*. **47,** 809-812.
508 Edmond J. M., Measures C., Mangum B., Grant B., Sclater F. R., Collier R., Hudson A.,
509 Gordon L. I. and Corliss J. B. (1979) On the formation of metal-rich deposits at ridge
510 crests. *Earth Planet. Sci. Lett.* **46**, 19-30.
511 Fricke G. and Heilig K. (2004) *Nuclear Charge Radii (Landolt-Bornstein Numerical*
512 *Data and Functional Relationships in Science and Technology - New Series)* (ed.
513 Schopper H.) Springer, Berlin.
514 Frisch M. J., Trucks G. W., Schlegel H. B., Scuseria, G. E., Robb M. A., Cheeseman J.
515 R., Montgomery Jr. J. A., Vreven T., Kudin K. N., Burant J. C., Millam J. M.,
516 Iyengar S. S., Tomasi J., Barone V., Mennucci B., Cossi M., Scalmani G., Rega N.,
517 Petersson G. A., Nakatsuji H., Hada M., Ehara M., Toyota K., Fukuda R., Hasegawa
518 J., Ishida M., Nakajima T., Honda Y., Kitao O., Nakai H., Klene M., Li X., Knox J.
519 E., Hratchian H. P., Cross J. B., Adamo C., Jaramillo J., Gomperts R., Stratmann R.
520 E., Yazyev O., Austin A. J., Cammi R., Pomelli C., Ochterski J. W., Ayala P. Y.,
521 Morokuma K., Voth G. A., Salvado, P., Dannenberg J. J., Zakrzewski V. G.,
522 Dapprich S., Daniels A. D., Strain M. C., Farkas O., Malick D. K., Rabuck A. D.,

523 Raghavachari K., Foresman J. B., Ortiz J. V., Cui Q., Baboul A. G., Clifford S.,
524 Cioslowski J., Stefanov B. B., Liu G., Liashenko A., Piskorz P., Komaromi I., Martin
525 R. L., Fox D. J., Keith T., Al-Laham M. A., Peng C. Y., Nanayakkara A.,
526 Challacombe M., Gill P. M. W., Johnson B., Chen W., Wong M. W., Gonzalez C.,
527 and Pople J. A. (2003) *Gaussian 03*, *Revision B.05*, Gaussian, Inc.: Pittsburgh PA.
528 Fujii T., Moynier F., Uehara A., Abe M., Yin Q.-Z., Nagai T., and Yamana H. (2009a)
529 Mass-dependent and mass-independent isotope effects of zinc in a redox reaction. *J.*
530 *Phys. Chem. A* **113**, 12225-12232.
531 Fujii T., Moynier F., and Albarède F. (2009b) The nuclear field shift effect in chemical
532 exchange reactions. *Chem. Geol*. **267**, 139-156.
533 Fujii T., Moynier F., Telouk P., and Abe M. (2010) Experimental and theoretical
534 investigation of isotope fractionation of zinc between aqua, chloro, and macrocyclic
535 complexes. *J. Phys. Chem. A* **114**, 2543-2552.
536 Fujii T., Moynier F., Dauphas N. and Abe M. (2011) Theoretical and experimental
537 investigation of nickel isotopic fractionation in species relevant to modern and
538 ancient oceans. *Geochim. Cosmochim. Acta* **75**, 469-482.
539 Fujii T., Moynier F., Agranier A., Ponzevera E., and Abe M. (in press) Isotope
540 fractionation of palladium in chemical exchange reaction. *Proc. Radiochim. Acta*.
541 DOI 10.1524/rcpr.2011.0060.
542 Hayashi K., Sugaki A., and Kitakaze A (1990) Solubility of sphalerite in aqueous
543 sulfide solutions at temperatures between 25 and 240°C. *Geochim. Cosmochim. Acta*
544 **54**, 715-725.

545 Hulme S. M., Wheat C. G., Fryer P., Mottl M. J., (2010) Pore water chemistry of the
546 Mariana serpentinite mud volcanoes: A window to the seismogenic zone. *Geochem.*
547 *Geophys. Geosys.*, **11**, Q01X09.
548 Irish D. E., MCCarroll B. and Young T. F. (1963) Raman study of zinc chloride
549 solutions. *J. Chem. Phys*. **39**, 3436-3444.
550 John S. G., Rouxel O. J., Craddock P. R., Engwall A. M. and Boyle E. A. (2008) Zinc
551 stable isotopes in seafloor hydrothermal vent fluids and chimneys. *Earth Planet. Sci.*
552 *Lett.* **269**, 17-28.
553 Kavner A., John S. G., Sass S., and Boyle E. A., (2008) Redox-driven stable isotope
554 fractionation in transition metals: Application to Zn electroplating. *Geochim.*
555 *Cosmochim. Acta* **72**, 1731–1741.
556 Kelley K. D., Wilkinson J. J., Chapman J. B., Crowther H. L.and Weiss D. J. (2009)
557 Zinc isotopes in sphalerite from base metal deposits in the red dog district, northern
558 Alaska. *Economic Geol*. **104**, 767-773.
559 King W. H. (1984) *Isotope Shifts in Atomic Spectra*; Plenum Press, New York.
560 Lee C. T., Yang W. T., and Parr R. G. (1988) Development of the colle-salvetti
561 correlation-energy formula into a functional of the electron-density. *Phys. Rev. B* **37**,
562 785-789.
563 Li J., Fisher C. L., Chen J. L., Bashford D., and Noodleman, L. (1996) Calculation of
564 redox potentials and pK_a values of hydrated transition metal cations by a combined
565 density functional and continuum dielectric theory. *Inorg. Chem.* **35**, 4694-4702.
566 Luther G. W. III, Rickard D. T., Theberge S., and Olroyd A. (1996) Determination of
567 metal (bi)sulfide stability constants of Mn^{2+}, Fe^{2+}, Co^{2+}, Ni^{2+}, Cu^{2+}, and Zn^{2+} by
568 voltammetric methods. *Environ. Sci. Technol*. **30**, 671-679.

569 Luther G. W. III, Theberge S. M., and Rickard D. T. (1999) Evidence for aqueous
570 clusters as intermediates during zinc sulfide formation. *Geochim. Cosmochim. Acta*
571 **63**, 3159-3169.
572 Luther G. W. III and Rickard D. T. (2005) Metal sulfide cluster complexes and their
573 biogeochemical importance in the environment. *J. Nanoparticle Res*. **7**, 389-407.
574 Maeda M., Ito T., Hori M., Johansson G. (1995) The structure of zinc chloride
575 complexes in aqueous solution. *Z. Naturforsch*. **51a**, 63-70.
576 Macleod G., Mcneown C., Hall A. J., and Russel M. J. (1994) Hydrothermal and
577 oceanic pH conditions of possible relevance to the origin of life. *Origin Life Evol.*
578 *Biosphere* **24**, 19-41.
579 Maréchal C. N., Douchet C., Nicolas E. and Albarède F. (2000) The abundance of zinc
580 isotopes as a marine biogeochemical tracer. *Geochem. Geophys. Geosyst.* **1**,
581 1999GC-000029
582 Maréchal C. and Albarède F. (2002) Ion-exchange fractionation of copper and zinc
583 isotopes. *Geochim. Cosmochim. Acta* **66**, 1499-1509.
584 Mason T. F. D., Weiss D. J., Chapman J. B., Wilkinson J. J., Tessalina S. G., Spiro B.,
585 Horstwood M. S. A., Spratt J., Coles B. J. (2005) Zn and Cu isotopic variability in the
586 Alexandrinka volcanic-hosted massive sulphide (VHMS) ore deposit, Urals, Russia.
587 *Chem. Geol*., **221**, 170-187.
588 Matsubara E. and Waseda Y (1989) An anomalous x-ray scattering study of an aqueous
589 solution of $ZnC1_2$. *J. Phys. Condens. Matter* **l**, 8575-8582.
590 Mink J., Németh Cs., Hajba L., Sandström, M. and Goggin P. L. (2003) Infrared and
591 Raman spectroscopic and theoretical studies of hexaaqua metal ions in aqueous
592 solution. *J. Mol. Struct.* **661-662**, 141-151.

593 Mottl M. J., Wheat C. G., Fryer P., Gharib J., and Martin J. B. (2004) Chemistry of
594 springs across the Mariana forearc shows progressive devolatilization of the
595 subducting plate. *Geochim. Cosmochim. Acta* **68**, 4915-4933.
596 Nomura M., Higuchi N., and Fujii Y. (1996) Mass dependence of uranium isotope
597 effects in the U(IV)-U(VI) exchange reaction. *J. Am. Chem. Soc*. **118**, 9127-9130.
598 Patterson, C. S. Slocum, G. H. Busey, R. H. and Mesmer, R. E., (1982) Carbonate
599 equilibria in hydrothermal systems: first ionization of carbonic acid in NaCl media to
600 300˚C. *Geochim. Cosmochim. Acta* **46**, 1653-1663.
601 Patterson, C. S., Busey, R. H. and Mesmer, R. E. (1984) Second ionization of carbonic
602 acid in NaCl media to 250˚C. *J. Soln. Chem.* **13**, 647-661.
603 Read A. J. (1975) The first ionization constant of carbonic acid from 25 to 250˚C and to
604 2000 bar. *J. Soln. Chem*. **4**, 53-70.
605 Pichat, S., Douchet, C. and Albarède, F. (2003) Zinc isotope variations in deep-sea
606 carbonates from the eastern equatorial Pacific over the last 175 ka. *Earth Planet. Sci.*
607 *Lett*. **210**, 167–178.
608 Pons M.L., Quitté G., Rosing M., Douchet C., Reynard B., Mills R. and Albarède F.
609 (2010) Serpentinization at Isua, a forearc environment identified by Zn isotopes.
610 *AGU Fall Meeting*, Abstract B41B-0306.
611 Ruaya J. R. and Seward T. M. (1986) The stability of chlorozinc(II) complexes in
612 hydrothermal solutions up to 350°C. *Geochim. Cosmochim. Acta* **50**, 651-661.
613 Rickard D. and Luther G. W. III (2006) Metal sulfide complexes and clusters. *Rev.*
614 *Mineoral. Geochem*., **61**, 421-504.
615 Rose N. M., Rosing, M. T., Bridgwater D. (1996) The origin of metacarbonate rocks in
616 the Archaean Isua supracrustal belt west Greenland. *Amer. J. Sci.*, **296**, 1004-1044.

617 Rudolph W. W. and Pye C. C. (1999) Zinc(II) hydration in aqueous solution. A Raman
618 spectroscopic investigation and an *ab-initio* molecular orbital study. *Phys. Chem.*
619 *Chem. Phys*. **1**, 4583-4593.
620 Rulíšek L. and Havlas Z. (1999) Ab initio calculations of monosubstituted (CH_3OH,
621 CH_3SH, NH_3) hydrated ions of Zn^{2+} and Ni^{2+}. *J. Phys. Chem. A* **103**, 1634-1639.
622 Rustad J. R., Casey W. H., Yin Q.-Z., Bylaska E. J., Felmy A. R., Bogatko S. A.,
623 Jackson V. E., Dixon D. A. (2010) Isotopic fractionation of Mg^{2+}(aq), Ca^{2+}(aq), and
624 Fe^{2+}(aq) with carbonate minerals. *Geochim. Cosmochim. Acta* **74**, 6301-6323.
625 Saito M. A., Sigman D. M., and Morel F. M. M. (2003) The bioinorganic chemistry of
626 the ancient ocean: the co-evolution of cyanobacterial metal requirements and
627 biogeochemical cycles at the Archean-Proterozoic boundary? *Geochim. Cosmochim.*
628 *Acta* **356**, 308-318.
629 Schauble E. A. (2003) Modeling zinc isotope fractionations. *Eos. Trans. AGU*, **84**, Fall
630 Meet. Suppl., Abstract B12B-0781.
631 Smith, R. W., Popp, C. J., and Norman, D. I. (1986) The dissociation of oxy-acids at
632 elevated temperatures. *Geochim. Cosmochim. Acta*, **50**, 137-142.
633 Stanley Jr. J. K. and Byrne R. H. (1990) Inorganic complexation of Zinc(II) in seawater.
634 *Geochim. Cosmochim. Acta* **54**, 753-760.
635 Suleimenov O. M and Seward T. M. (1997) A spectrophotometric study of hydrogen
636 sulphide ionisation in aqueous solutions to 350˚C. *Geochim. Cosmochim. Acta* **61**,
637 5187-5198.
638 Tagirov B. R., Suleimenov O. M., and Seward T.M. (2007) Zinc complexation in
639 aqueous sulfide solutions: Determination of the stoichiometry and stability of

640 complexes via $ZnS_{(cr)}$ solubility measurements at 100°C and 150 bars. *Geochim. Cosmochim. Acta* **71**, 4942–4953.
642 Tagirov B. R. and Seward T.M. (2010) Hydrosulfide/sulfide complexes of zinc to
643 250 °C and the thermodynamic properties of sphalerite. *Chem. Geol*. **269**, 301–311.
644 Tossell, J. A. (1991) Calculations of the structures, stabilities, and raman and Zn NMR
645 spectra of $ZnCl_n(OH_2)_a^{2-n}$ species in aqueous solution. *J. Phys. Chem*. **95**, 366-371.
646 Tossel J. A. and Vaughan D. J. (1993) Bisulfid complexes of zinc and cadmium in
647 aqueous solution: Calcultion of structure, stability, vibrational, and NMR spectra, and
648 of speciation on sulfide mineral surfaces. Geochim. Cosmochim. Acta 57, 1935-1945.
649 Turner D. R., Whitfield M. and Dickson A. G. (1981) The equilibrium speciation of
650 dissolved components in freshwater and sea water at 25°C and 1 atm pressure.
651 *Geochim. Cosmochim. Acta* **45**, 855-881.
652 Urey H. C. (1947) The thermodynamic properties of isotopic substances. *J. Chem. Soc.*
653 562-581.
654 Von Damm K. L. (1990) Seafloor hydrothermal activity: Black smoker chemistry and
655 chimnerys. *Annu. Rev. Earth. Planet. Sci*. **18**, 173-204.
656 Yamaguchi T., Hayashi S., and Ohtaki H. (1989) X-ray diffraction and raman studies of
657 zinc(II) chloride hydrate melts, $ZnCl{\bullet}RH_2O$ (R = 1.8, 2.5, 3.0, 4.0, and 6.2). *J. Phys.*
658 *Chem*. **93**, 2620-2625.
659 Zhang J. -Z. and Miller F. J. (1994) Investigation of metal sulfide complexes in sea
660 water using cathodic stripping square wave voltammetry. *Anal. Chim. Acta* **284**,
661 497-504.
662 Zirino A. and Tamamoto S. (1972) A pH-dependent model for the chemical speciation
663 of copper, zinc, cadmium, and lead in seawater. *Limnol. Oceanogr*. **17**, 661-671.

664

665

666

667

668

669

670 Table 1 Zn-O bond distances and ν_1 frequencies determined for hydrated Zn^{2+}.

Species	Method[a]	Zn-O (Å)	ν_1 (cm^{-1})	ν_2 (cm^{-1})	ν_3 (cm^{-1})	Reference
$Zn(H_2O)_6^{2+}$	DFT	2.128	333	-	-	Fujii et al. (2010)
$Zn(H_2O)_6^{2+}$	DFT[b]	2.128	333	219	294	This study
$Zn(H_2O)_6^{2+}$	DFT[c]	2.102	353	227	317	This study
$Zn(H_2O)_{18}^{2+}$	DFT[d]	2.114	380	-	-	Fujii et al. (2010)
$Zn(H_2O)_{18}^{2+}$	DFT[d]	2.114	380	298	362	This study
-	XRD	2.08	-	-	-	Tossel (1991)
-	XRD	2.15	-	-	-	Maeda et al. (1995)
-	AXN	2.10-2.15	-	-	-	Matsubara and Waseda (1989)
-	EXAFS	2.05-2.07	-	-	-	Dreier and Rabe (1986)
-	Raman	-	390±10	-	-	Irish et al. (1963)
-	Raman	-	379±5	-	-	Yamaguchi et al. (1989)
-	Raman	-	385	-	-	Maeda et al. (1995)
-	Raman, IR	-	390±2	270±5	365±5	Rudolph and Pye (1999)
-	Raman, IR	-	389	360	386	Mink et al. (2003)

671 [a] DFT (density functional theory), XRD (x-ray diffraction), AXN (anomalous x-ray scattering),
672 EXAFS (extended x-ray absorption fine structure), IR (infrared).
673 [b] DFT calculation results with various basis sets are given in electronic annex, Tables S1 and
674 S2.
675 [c] CPCM continuum solvation method was applied.
676 [d] 12 H_2O molecules were arranged around $Zn(H_2O)_6^{2+}$.

Table 2 Logarithm of the reduced partition function, ln β, for isotope pair $^{66}Zn/^{64}Zn$.

Species	ln β at 298K (‰)	ln β at 423K (‰)	ln β at 573K (‰)
$Zn(H_2O)_6^{2+}$ [a]	3.263 3.280[b]	1.659 1.660[b]	0.915 0.913[b]
$Zn(H_2O)_{18}^{2+}$ [a]	3.576	1.819	1.004
$Zn(HS)_2(H_2O)_4$	2.717	1.384	0.764
$Zn(HS)_3(H_2O)_2^-$	3.028	1.535	0.845
$Zn(HS)_4^{2-}$	2.190	1.101	0.604
$ZnS(HS)H_2O^-$	2.628	1.326	0.728
$ZnCl(H_2O)_5^+$ [a]	3.142	1.599	0.882
$ZnCl_2(H_2O)_4$ [a]	2.956	1.495	0.822
$ZnHCO_3(H_2O)_4^+$	3.439	1.754	0.969
$ZnCO_3(H_2O)_4$	3.990	2.050	1.137

[a] Calculated structures (Fujii et al., 2010) were reproduced.

[b] Applying the CPCM continuum solvation method.

690

691

692

693

694

695

696

697

698

699 Table 3 Bond distances calculated for Zn sulfides.

Species	Bond[a], Zn-O (Å)	Bond[a], Zn-S (Å)
$Zn(HS)_2(H_2O)_4$	2.434(2) 2.514(2)	2.295(2)
$Zn(HS)_3(H_2O)_2$	3.536(2)	2.300(2) 2.324(1)
$Zn(HS)_4$	–	2.450(4)
$ZnS(HS)H_2O^-$	3.412(2)[b]	2.331(2)[b] 2.365(1)

700 [a] Numbers of bonds are shown in parentheses.
701 [b] Shared with another Zn^{2+}.
702

Table 4 Stability constants of Zn sulfide and chloride systems.

	298K	423K	573K	Reference
log $K_{Zn(HS)_2}$	9.40	9.82	12.56[a]	Tagirov and Seward (2010)
log $K_{Zn(HS)_3^-}$	13.06[a]	12.39[b]	14.41[a]	Tagirov and Seward (2010)
log $K_{Zn(HS)_4^{2-}}$	14.47	12.02[a]	11.80[a]	Tagirov and Seward (2010)
log $K_{ZnS(HS)^-}$	3.41	2.69	2.47[a]	Tagirov and Seward (2010)
log K_{ZnCl^+}	–0.03[c]	2.89	6.53[c]	Ruaya and Seward (1986)
log K_{ZnCl_2}	0.13[c]	2.96	7.51[c]	Ruaya and Seward (1986)
log $K_{ZnHCO_3^+}$	2.1	2.1[d]	2.1[d]	Zirino and Yamamoto (1972)
log K_{ZnCO_3}	5.3	5.3[d]	5.3[d]	Zirino and Yamamoto (1972)
log $K_{HCO_3^-}$	–6.35	–6.74	–8.50	Smith et al. (1986)
log $K_{CO_3^{2-}}$	–16.69	–16.98	–19.82	Smith et al. (1986)
pK_a	6.99	6.49	7.89	Suleimenov and Seward (1997)

[c] Values are shown in Appendix C in Tagirov and Seward (2010).
[b] Value for 373K was used. The value for 423K did not reproduce the speciation calculation of Tagirov and Seward (2010).
[c] Calculated from equation 23 in Ruaya and Seward (1986).
[d] Stability constants at 298 K.

726 **Figure captions**

727 **Figure 1 Molecular structures of hydrated Zn^{2+} and aqueous Zn sulfides.** Structures
728 are drawn by using GaussView3.0 (Gaussian Inc.). a) $Zn(H_2O)_6^{2+}$, b) $Zn(HS)_2(H_2O)_4$, c)
729 $Zn(HS)_3(H_2O)_2^-$, d) $Zn(HS)_4^{2-}$, e) $Zn_2S_2(HS)_2(H_2O)_2^{2-}$ = $2[ZnS(HS)(H_2O)^-]$, f)
730 $ZnHCO_3(H_2O)_4^+$, and g) $ZnCO_3(H_2O)_4$.

731 **Figure 2 Temperature dependence of ln β.** The ln β values shown in Table 2 are fitted
732 by linear functions of T^{-2}.

733 **Figure 3 Mole fractions of Zn species and Zn isotopic variations as functions of pH**
734 **at 298 K.** a) Mole fractions of Zn species in Cl^- and carbonate free hydrous fluid under
735 Σ[S]=0.1 M, b) Mole fractions of Zn species with Σ[S]=5 mM and $[Cl^-]$ = 0.55 M under
736 P_{CO_2} = 50 bar, c) Species $\delta^{66}Zn$ relative to the bulk solution in Cl^- and carbonate free
737 hydrous fluid, and d) $\delta^{66}Zn$ under the hydrothermal condition of b). Dotted lines at 0‰
738 in c) and d) show $\delta^{66}Zn$ of bulk solution (averaged $\delta^{66}Zn$ in the whole solution). Σ[Zn]
739 was set to be $10^{-6.1}$ M (Tagirov and Seward, 2010).

740 **Figure 4 Mole fractions of Zn species and Zn isotopic variations as functions of pH**
741 **at 423 K. Panels a-d : see caption of Fig. 3.** Mole fraction of Zn^{2+} in Fig. 4b is 0.14%
742 at pH=2 and smaller than that at pH>2. The maximum value of $Zn(HS)_4^{2-}$ mole fraction
743 is 0.06% at pH=7.1 (Fig. 4b). Dotted lines in c) and d) mean $\delta^{66}Zn$ of bulk solution
744 (averaged $\delta^{66}Zn$ in the whole solution). Σ[Zn] was set to be $10^{-6.1}$ M (Tagirov and
745 Seward, 2010).

746 **Figure 5 Mole fractions of Zn species and Zn isotopic variations as functions of pH**
747 **at 573 K. Panels a-d : see caption of Fig. 3.** Mole fraction of Zn^{2+} in Fig. 5b is smaller
748 than 0.001%. The maximum value of $Zn(HS)_4^{2-}$ mole fraction is 0.02% (Fig. 5a) or

749 0.0002% (Fig. 5b) at pH=9.3. The maximum value of $ZnHCO_3^+$ mole fraction is 0.1%
750 at pH= 10.5 (Fig. 5b). Dotted lines in c) and d) mean $\delta^{66}Zn$ of bulk solution (averaged
751 $\delta^{66}Zn$ in the whole solution). Σ[Zn] was set to be $10^{-6.1}$ M (Tagirov and Seward, 2010).
752
753
754
755

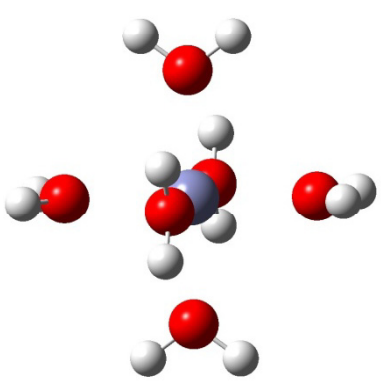

a) $Zn(H_2O)_6^{2+}$

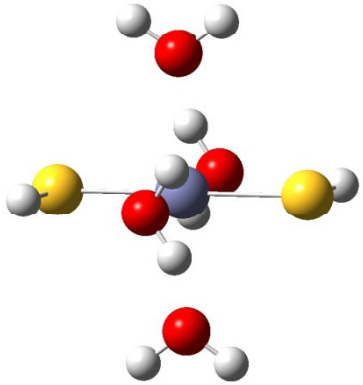

b) $Zn(HS)_2(H_2O)_4$

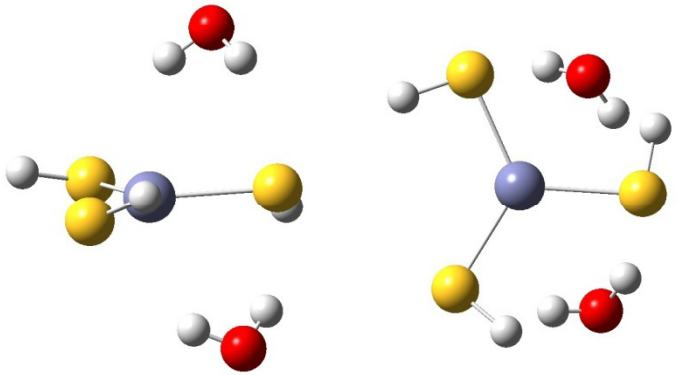

c) $Zn(HS)_3(H_2O)_2^-$: side view (left), top view (right)

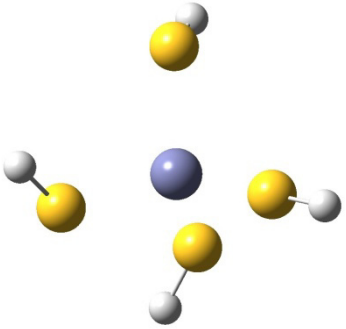

d) $Zn(HS)_4^{2-}$

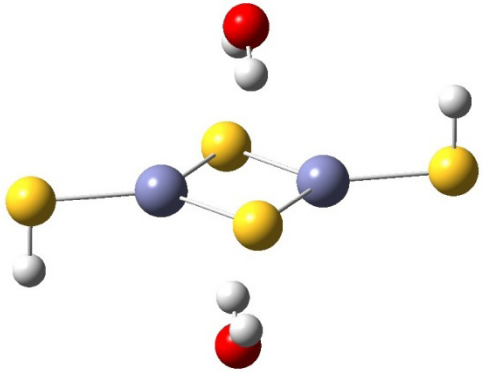

e) $Zn_2S_2(HS)_2(H_2O)_2^{2-}$
= $2[ZnS(HS)H_2O^-]$

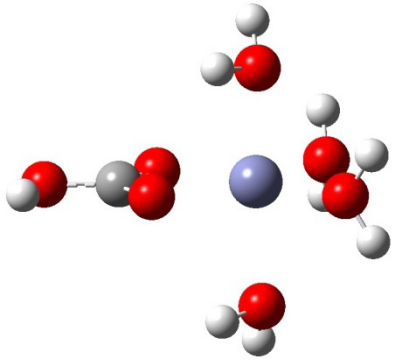

f) $ZnHCO_3(H_2O)_4^+$

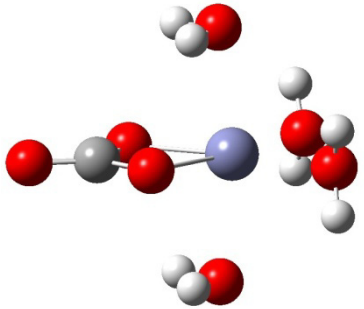

g) $ZnCO_3(H_2O)_4$

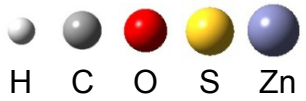

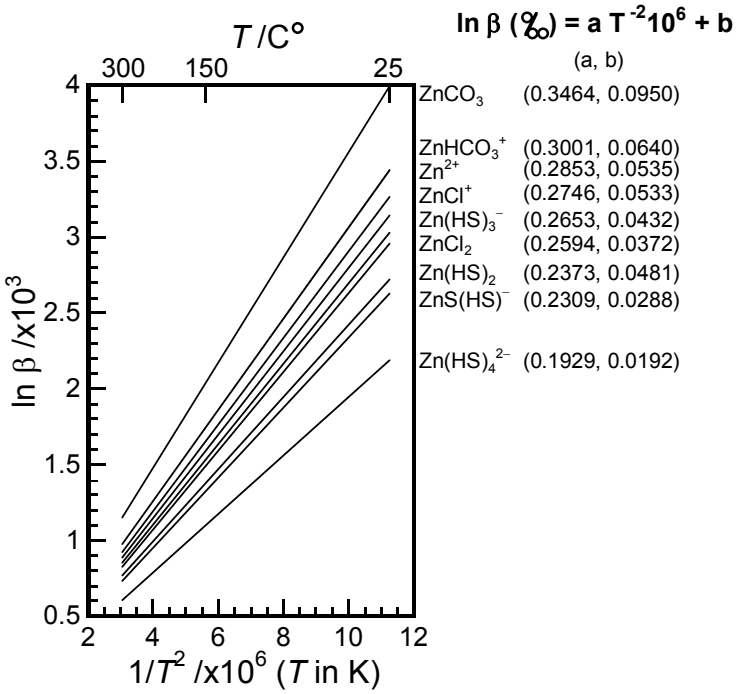
T /C°
300
150
25
4
3.5
3
2.5
2
1.5
1
0.5
ln β /x10^3
2
4
6
8
10
12
1/T^2 /x10^6 (T in K)
ln β (‰) = a T^-2 10^6 + b
(a, b)
ZnCO3 (0.3464, 0.0950)
ZnHCO3+ (0.3001, 0.0640)
Zn2+ (0.2853, 0.0535)
ZnCl+ (0.2746, 0.0533)
Zn(HS)3− (0.2653, 0.0432)
ZnCl2 (0.2594, 0.0372)
Zn(HS)2 (0.2373, 0.0481)
ZnS(HS)− (0.2309, 0.0288)
Zn(HS)4 2− (0.1929, 0.0192)

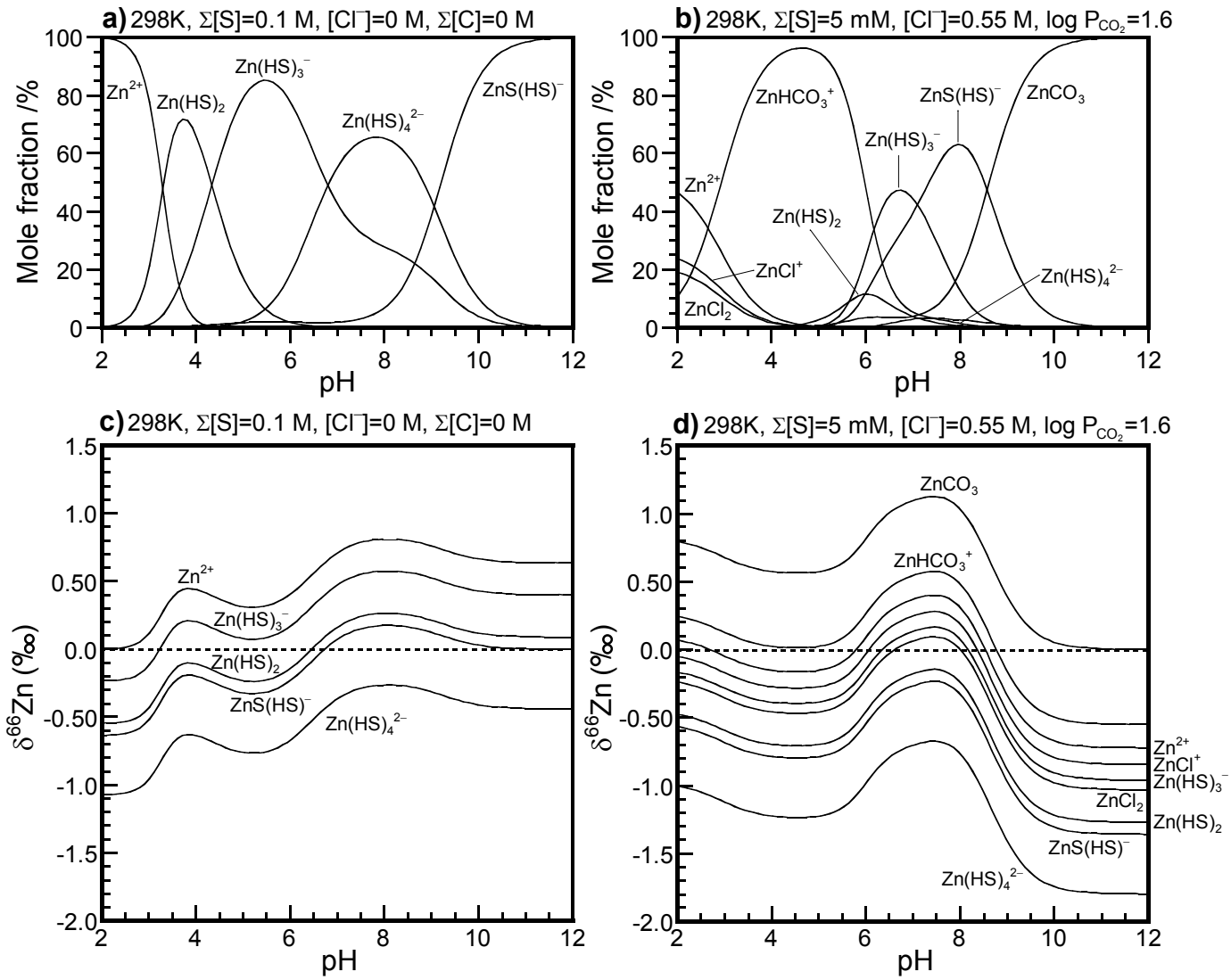
a) 298K, Σ[S]=0.1 M, [Cl⁻]=0 M, Σ[C]=0 M
Mole fraction /%
pH
Zn2+
Zn(HS)2
Zn(HS)3−
Zn(HS)4 2−
ZnS(HS)−
b) 298K, Σ[S]=5 mM, [Cl⁻]=0.55 M, log PCO2=1.6
Mole fraction /%
pH
ZnHCO3+
ZnS(HS)−
ZnCO3
Zn(HS)3−
Zn2+
Zn(HS)2
ZnCl+
ZnCl2
Zn(HS)4 2−
c) 298K, Σ[S]=0.1 M, [Cl⁻]=0 M, Σ[C]=0 M
δ66Zn (‰)
pH
Zn2+
Zn(HS)3−
Zn(HS)2
ZnS(HS)−
Zn(HS)4 2−
d) 298K, Σ[S]=5 mM, [Cl⁻]=0.55 M, log PCO2=1.6
δ66Zn (‰)
pH
ZnCO3
ZnHCO3+
Zn2+
ZnCl+
Zn(HS)3−
ZnCl2
Zn(HS)2
ZnS(HS)−
Zn(HS)4 2−

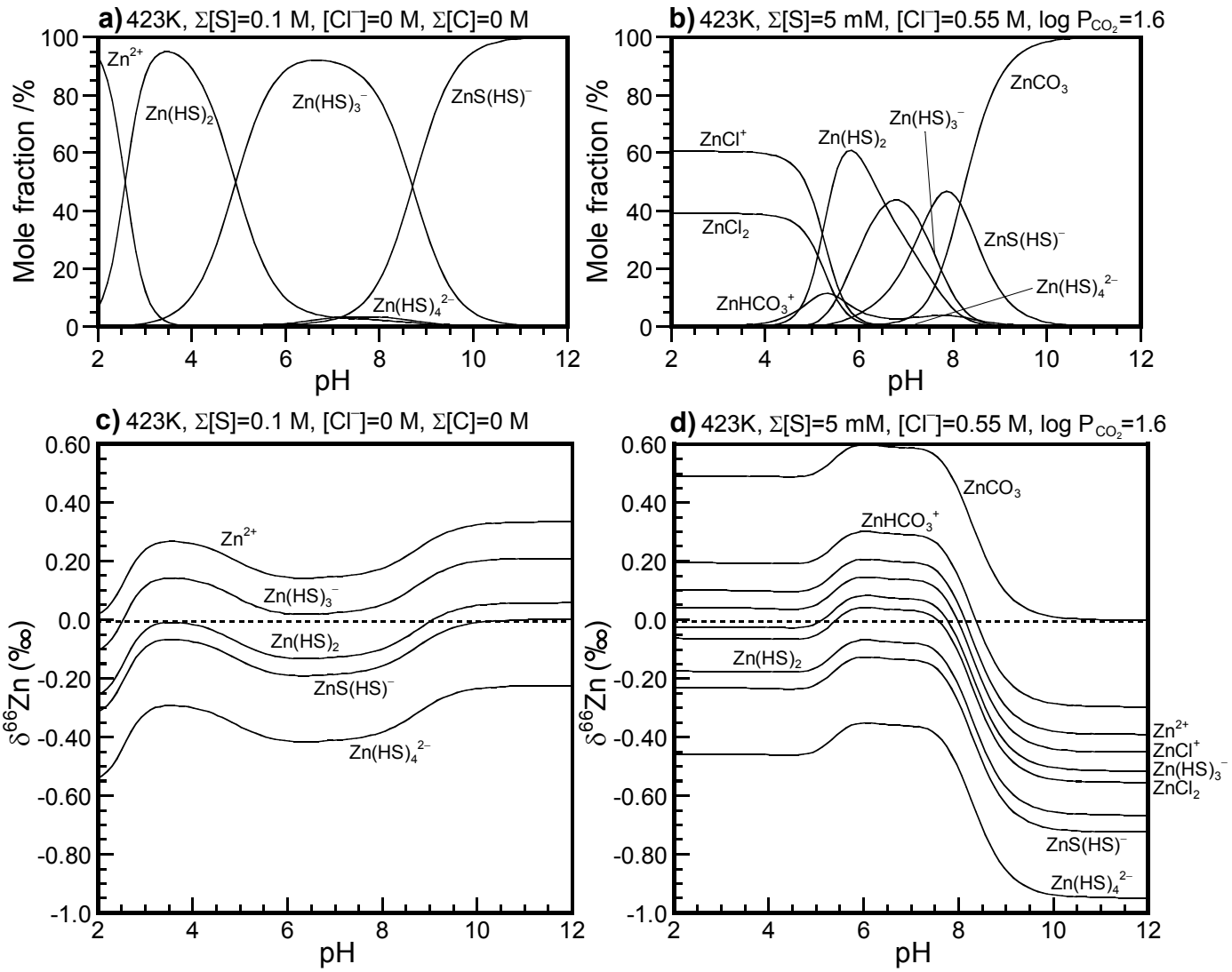
a) 423K, Σ[S]=0.1 M, [Cl⁻]=0 M, Σ[C]=0 M
Mole fraction /%
pH
Zn2+
Zn(HS)2
Zn(HS)3−
ZnS(HS)−
Zn(HS)4 2−
b) 423K, Σ[S]=5 mM, [Cl⁻]=0.55 M, log PCO2=1.6
Mole fraction /%
pH
ZnCO3
Zn(HS)3−
ZnCl+
Zn(HS)2
ZnCl2
ZnS(HS)−
ZnHCO3+
Zn(HS)4 2−
c) 423K, Σ[S]=0.1 M, [Cl⁻]=0 M, Σ[C]=0 M
δ66Zn (‰)
pH
Zn2+
Zn(HS)3−
Zn(HS)2
ZnS(HS)−
Zn(HS)4 2−
d) 423K, Σ[S]=5 mM, [Cl⁻]=0.55 M, log PCO2=1.6
δ66Zn (‰)
pH
ZnCO3
ZnHCO3+
Zn(HS)2
Zn2+
ZnCl+
Zn(HS)3−
ZnCl2
ZnS(HS)−
Zn(HS)4 2−

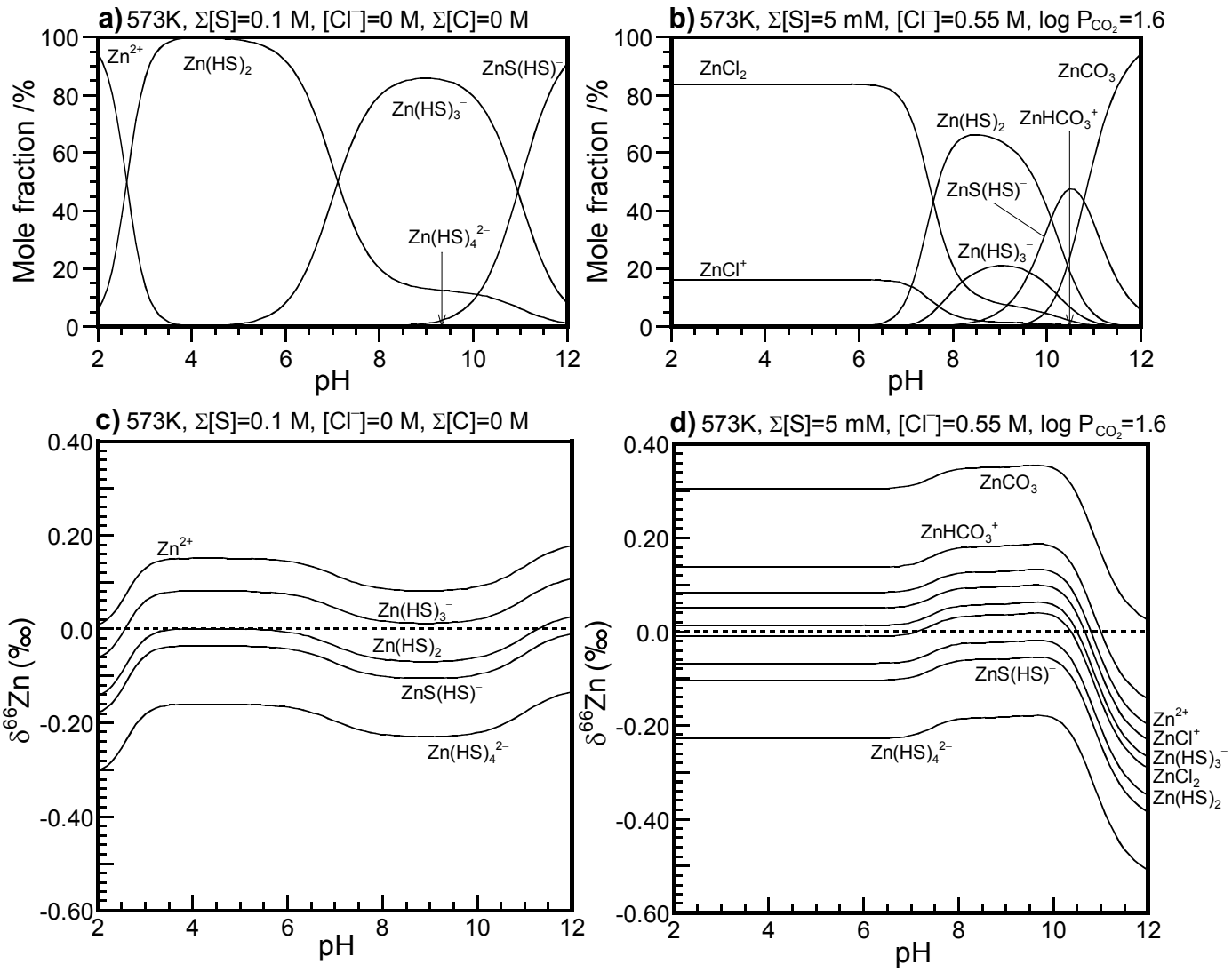
a) 573K, Σ[S]=0.1 M, [Cl⁻]=0 M, Σ[C]=0 M
Mole fraction /%
pH
Zn2+
Zn(HS)2
Zn(HS)3−
ZnS(HS)−
Zn(HS)4 2−
b) 573K, Σ[S]=5 mM, [Cl⁻]=0.55 M, log PCO2=1.6
ZnCl2
ZnCO3
Zn(HS)2
ZnHCO3+
ZnS(HS)−
Zn(HS)3−
ZnCl+
c) 573K, Σ[S]=0.1 M, [Cl⁻]=0 M, Σ[C]=0 M
δ66Zn (‰)
d) 573K, Σ[S]=5 mM, [Cl⁻]=0.55 M, log PCO2=1.6
Zn2+
ZnCl+
Zn(HS)3−
ZnCl2
Zn(HS)2

Supplementary material

The origin of Zn Isotope Fractionation in Sulfides

Toshiyuki Fujii[1], Frédéric Moynier[2], Marie-Laure Pons[3], and Francis Albarède[3]

[1] Research Reactor Institute, Kyoto University, 2-1010 Asashiro Nishi, Kumatori, Sennan Osaka 590-0494, Japan

[2] Department of Earth and Planetary Sciences and McDonnell Center for Space Sciences, Washington University in St. Louis, Campus Box 1169, 1 Brookings Drive, Saint Louis, MO 63130-4862, USA

[3] Ecole Normale Supérieure de Lyon, Université de Lyon 1, CNRS, 46, Allee d'Italie, 69364 Lyon Cedex 7, France

In order of appearance:

Figure S1: $Zn(H_2O)_6^{2+}$ with T_h symmetry and its vibrational modes, ν_1, ν_2, and ν_3

Table S1: Zn-O and O-H bond lengths and ∠HOH angles

Table S2: ν_1, ν_2, and ν_3 frequencies

Table S3: ln β's at 298 K

Figure S2: Mole fractions of Zn species and Zn isotopic variations as functions of pH at 573 K (for stronger complexation of Zn carbonates).

Figure S3: Mole fractions of Zn species and Zn isotopic variations as functions of pH at 298 K (Σ[S] = 0.1 M, $[Cl^-]$ = 0.55 M, and Σ[C] = 0 M).

Figure S4: Mole fractions of Zn species and Zn isotopic variations as functions of pH at 423 K (Σ[S] = 0.1 M, $[Cl^-]$ = 0.55 M, and Σ[C] = 0 M).

Figure S5: Mole fractions of Zn species and Zn isotopic variations as functions of pH at 573 K (Σ[S] = 0.1 M, $[Cl^-]$ = 0.55 M, and Σ[C] = 0 M).

Figure S6: Mole fractions of Zn species and Zn isotopic variations as functions of pH at 298 K (Σ[S] = 10 μM, $[Cl^-]$ = 0.55 M, and $\log P_{CO2} = -3.4$).

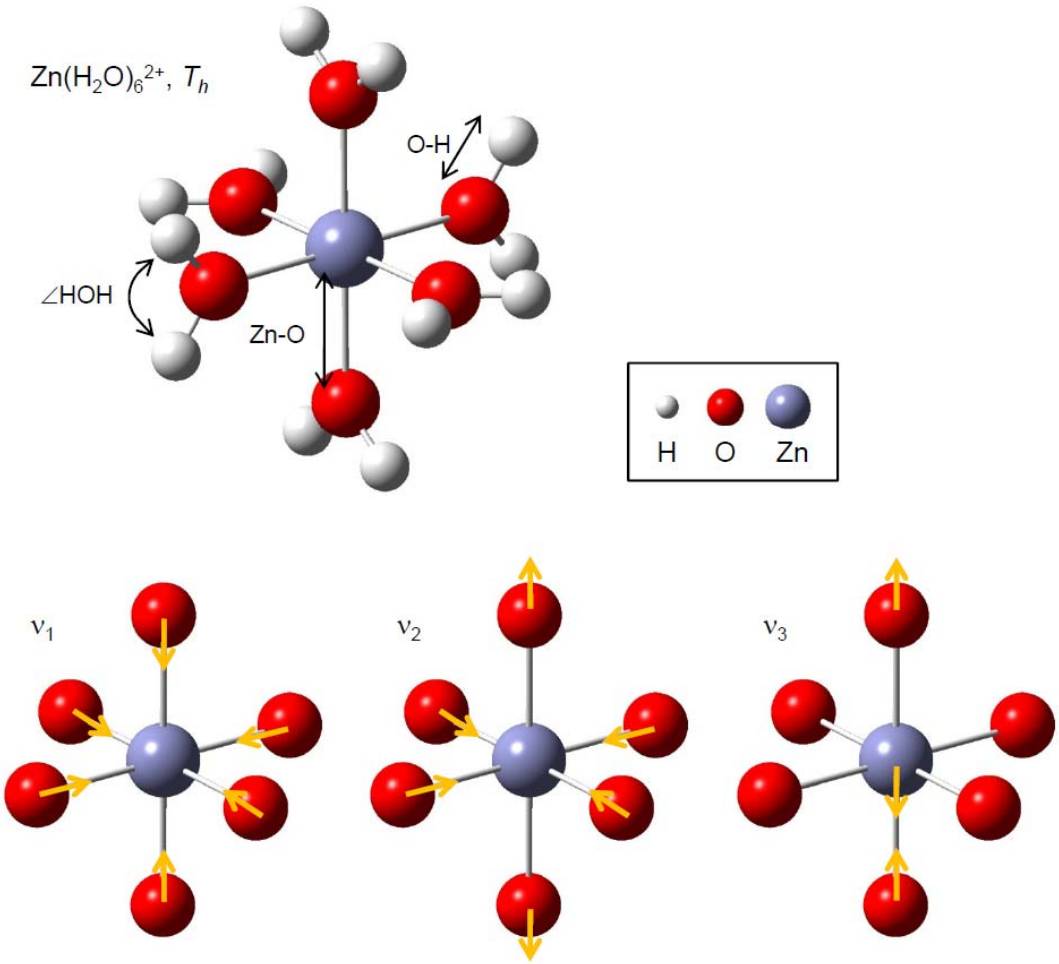

Fig. S1 $Zn(H_2O)_6^{2+}$ with T_h symmetry and its vibrational modes, ν_1, ν_2, and ν_3. Structures are drawn by using GaussView3.0 (Gaussian Inc.).

Table S1
Zn-O and O-H bond lengths and ∠HOH angles

Theory/Basis sets[a]	Zn-O (Å)	O-H (Å)	∠HOH (˚)
B3LYP			
6-31G(d)	2.094	0.973	107.2
6-31G(d,p)	2.092	0.969	107.4
6-31+G(d)	2.124	0.974	107.4
6-31+G(d,p)	2.125	0.970	107.6
6-31++G(d,p)	2.125	0.970	107.6
6-311G(d)	2.095	0.965	108.4
6-311G(d,p)	2.097	0.966	107.3
6-311+G(d)	2.118	0.966	108.2
6-311+G(d,p)	2.128	0.967	107.4
6-311++G(d,p)	2.128	0.967	107.4
LanL2DZ & 6-31G(d)	2.131	0.973	107.1
LanL2DZ & 6-31G(d,p)	2.131	0.968	107.1
LanL2DZ & 6-31+G(d)	2.143	0.974	107.1
LanL2DZ & 6-31+G(d,p)	2.145	0.970	107.3
LanL2DZ & 6-31++G(d,p)	2.146	0.970	107.3
LanL2DZ & 6-311G(d)	2.131	0.965	108.3
LanL2DZ & 6-311G(d,p)	2.138	0.966	107.1
LanL2DZ & 6-311+G(d)	2.135	0.966	108.0
LanL2DZ & 6-311+G(d,p)	2.146	0.967	107.1
LanL2DZ & 6-311++G(d,p)	2.146	0.967	107.1
UHF			
LanL2DZ & 6-31G(d)	2.142	0.954	107.3

[a] Orbital geometries and vibrational frequencies of aqueous Zn(II) species were computed using density functional theory (DFT) as implemented by the Gaussian03 code (Frisch et al., 2003). The DFT method employed here is a hybrid density functional consisting of Becke's three-parameter non-local hybrid exchange potential (B3) (Becke, 1993) with Lee-Yang and Parr (LYP) (Lee et al., 1988) non-local functionals. 6-31G and 6-311G basis set, which are all-electron basis sets, were chosen for H, O, and Zn. For comparison, an effective-core potential (ECP) basis set, LanL2DZ (Hay and Wadt, 1985a, b; Wadt and Hay, 1985), was tested for Zn. Unrestricted Hartree-Fock (UHF) theory was also tested.

Table S2
ν_1, ν_2, and ν_3 frequencies

Theory/Basis sets	ν_1 (cm^{-1})	ν_2 (cm^{-1})	ν_3 (cm^{-1})
B3LYP			
6-31G(d)	361	236	295
6-31G(d,p)	361	235	300
6-31+G(d)	336	217	290
6-31+G(d,p)	334	215	289
6-31++G(d,p)	335	216	289
6-311G(d)	372	246	339
6-311G(d,p)	371	244	334
6-311+G(d)	340	228	308
6-311+G(d,p)	333	219	294
6-311++G(d,p)	333	219	294
LanL2DZ & 6-31G(d)	338	243	301
LanL2DZ & 6-31G(d,p)	338	243	309
LanL2DZ & 6-31+G(d)	327	234	306
LanL2DZ & 6-31+G(d,p)	325	231	304
LanL2DZ & 6-31++G(d,p)	325	231	304
LanL2DZ & 6-311G(d)	342	250	329
LanL2DZ & 6-311G(d,p)	337	245	319
LanL2DZ & 6-311+G(d)	335	244	323
LanL2DZ & 6-311+G(d,p)	328	236	311
LanL2DZ & 6-311++G(d,p)	328	236	311
UHF			
LanL2DZ & 6-31G(d)	336	234	309

Table S3:
ln β's at 298 K

Theory/Basis sets	ln β (‰)
B3LYP	
6-31G(d)	3.427
6-31G(d,p)	3.405
6-31+G(d)	3.274
6-31+G(d,p)	3.215
6-31++G(d,p)	3.214
6-311G(d)	4.190
6-311G(d,p)	4.044
6-311+G(d)	3.501
6-311+G(d,p)	3.250
6-311++G(d,p)	3.239
LanL2DZ & 6-31G(d)	3.753 (3.74[a])
LanL2DZ & 6-31G(d,p)	3.732
LanL2DZ & 6-31+G(d)	3.520
LanL2DZ & 6-31+G(d,p)	3.465
LanL2DZ & 6-31++G(d,p)	3.474
LanL2DZ & 6-311G(d)	4.085
LanL2DZ & 6-311G(d,p)	3.838
LanL2DZ & 6-311+G(d)	3.859
LanL2DZ & 6-311+G(d,p)	3.600
LanL2DZ & 6-311++G(d,p)	3.598
UHF	
LanL2DZ & 6-31G(d)	3.594 (3.58[a])

[a] Black et al. (2011)

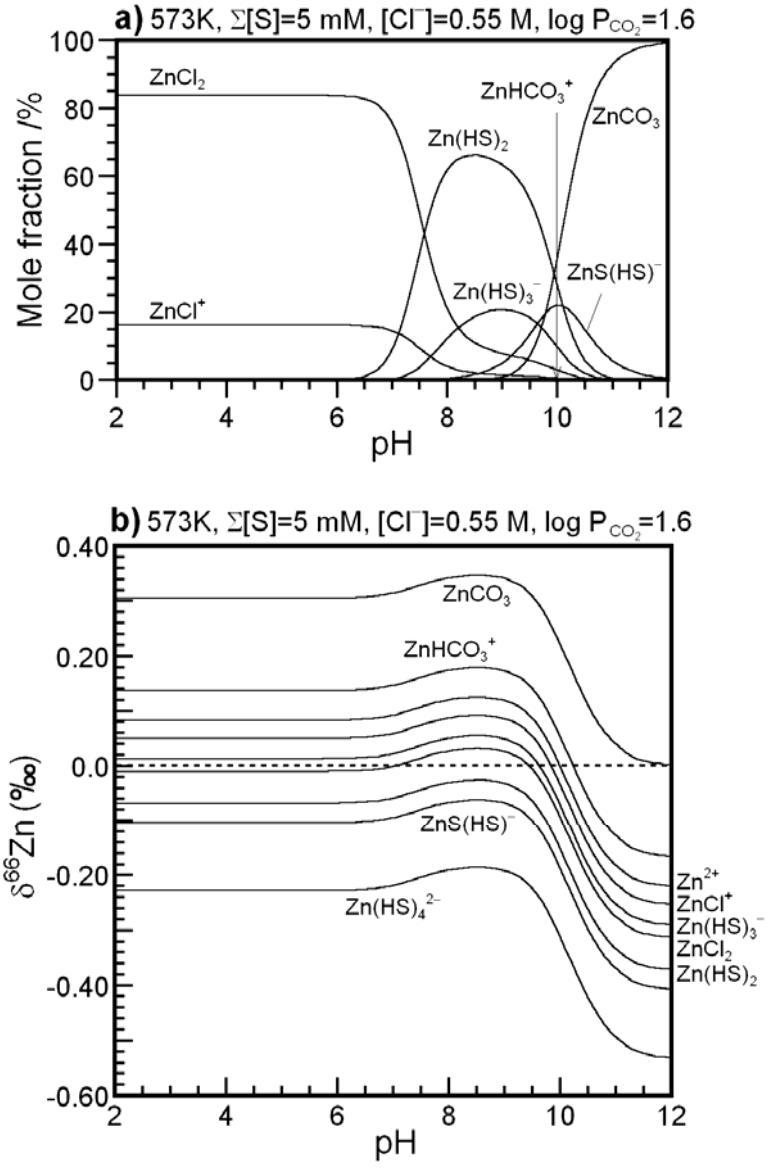

Fig. S2. Mole fractions of Zn species and Zn isotopic variations as functions of pH at 573 K (for stronger complexation of Zn carbonates). a) Mole fractions of Zn species with Σ[S]=5 mM and [Cl$^-$] = 0.55 M under P_{CO2} = 50 bar, b) δ^{66}Zn under the hydrothermal condition. Under an assumption that formations of $ZnHCO_3^+$ and $ZnCO_3$ are enhanced by increasing temperature, $K_{ZnHCO_3^+}$ and K_{ZnCO_3} were multiplied by 10 (as an example) and log $K_{ZnHCO_3^+}$ = 3.1 and log K_{ZnCO_3} = 6.3 were used. Mole fraction of Zn^{2+} in Fig. S2b is smaller than 0.001%. The maximum value of $Zn(HS)_4^{2-}$ mole fraction is 0.0002% at pH=9.3. The maximum value of $ZnHCO_3^+$ mole fraction is 0.5% at pH= 10.0. Dotted line in b) means δ^{66}Zn of bulk solution (averaged δ^{66}Zn in the whole solution). Σ[Zn] was set to be $10^{-6.1}$ M (Tagirov and Seward, 2010).

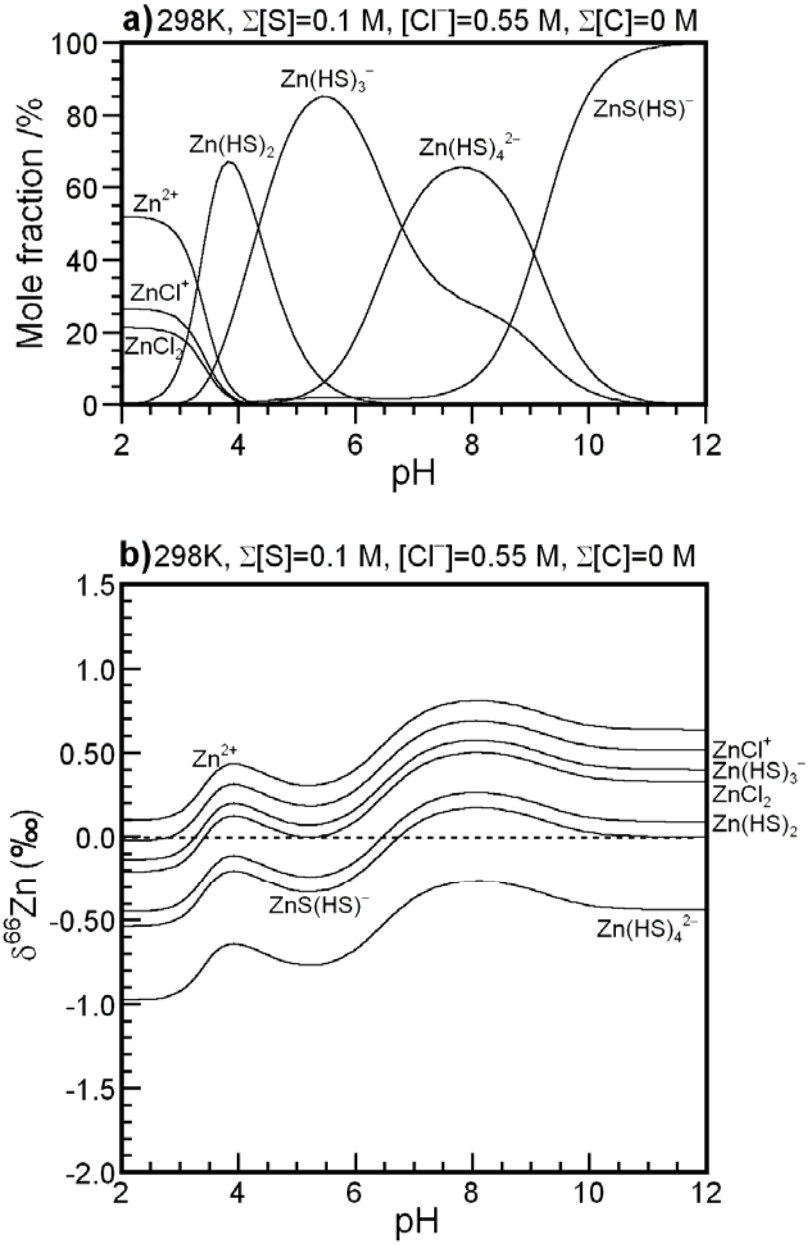

Fig. S3

Mole fractions of Zn species and Zn isotopic variations as functions of pH at 298 K (Σ[S] = 0.1 M, [Cl^-] = 0.55 M, and Σ[C] = 0 M). a) Mole fractions of Zn species in carbonate free hydrous fluid under Σ[S]=0.1 M and [Cl^-] = 0.55 M, b) δ^{66}Zn in carbonate free hydrous fluid. Dotted line in b) means δ^{66}Zn of bulk solution (averaged δ^{66}Zn in the whole solution). Σ[Zn] was set to be $10^{-6.1}$ M (Tagirov and Seward, 2010).

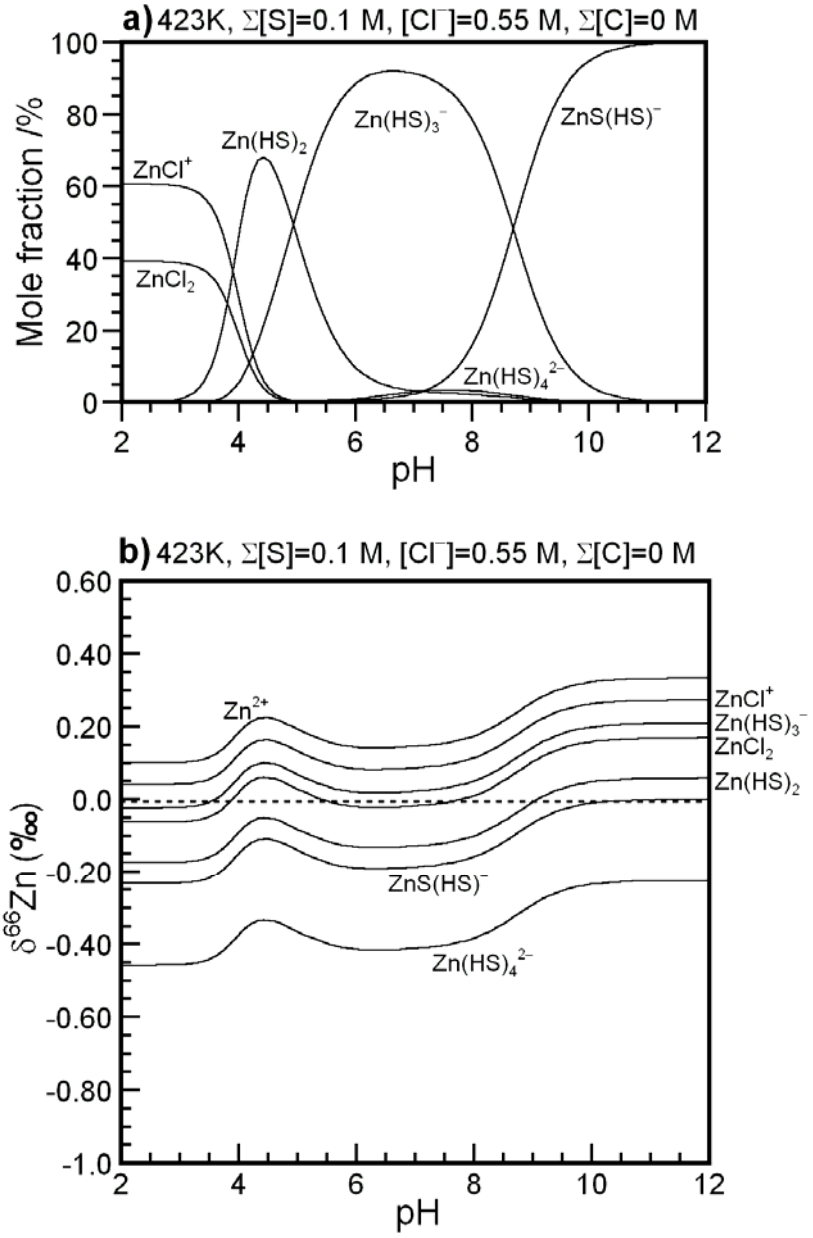

Fig. S4

Mole fractions of Zn species and Zn isotopic variations as functions of pH at 423 K (Σ[S] = 0.1 M, [Cl^-] = 0.55 M, and Σ[C] = 0 M). a) Mole fractions of Zn species in carbonate free hydrous fluid under Σ[S]=0.1 M and [Cl^-] = 0.55 M, b) δ^{66}Zn in carbonate free hydrous fluid. Mole fraction of Zn^{2+} is 0.14% at pH=2 and smaller than that at pH>2. Dotted line in b) means δ^{66}Zn of bulk solution (averaged δ^{66}Zn in the whole solution). Σ[Zn] was set to be $10^{-6.1}$ M (Tagirov and Seward, 2010).

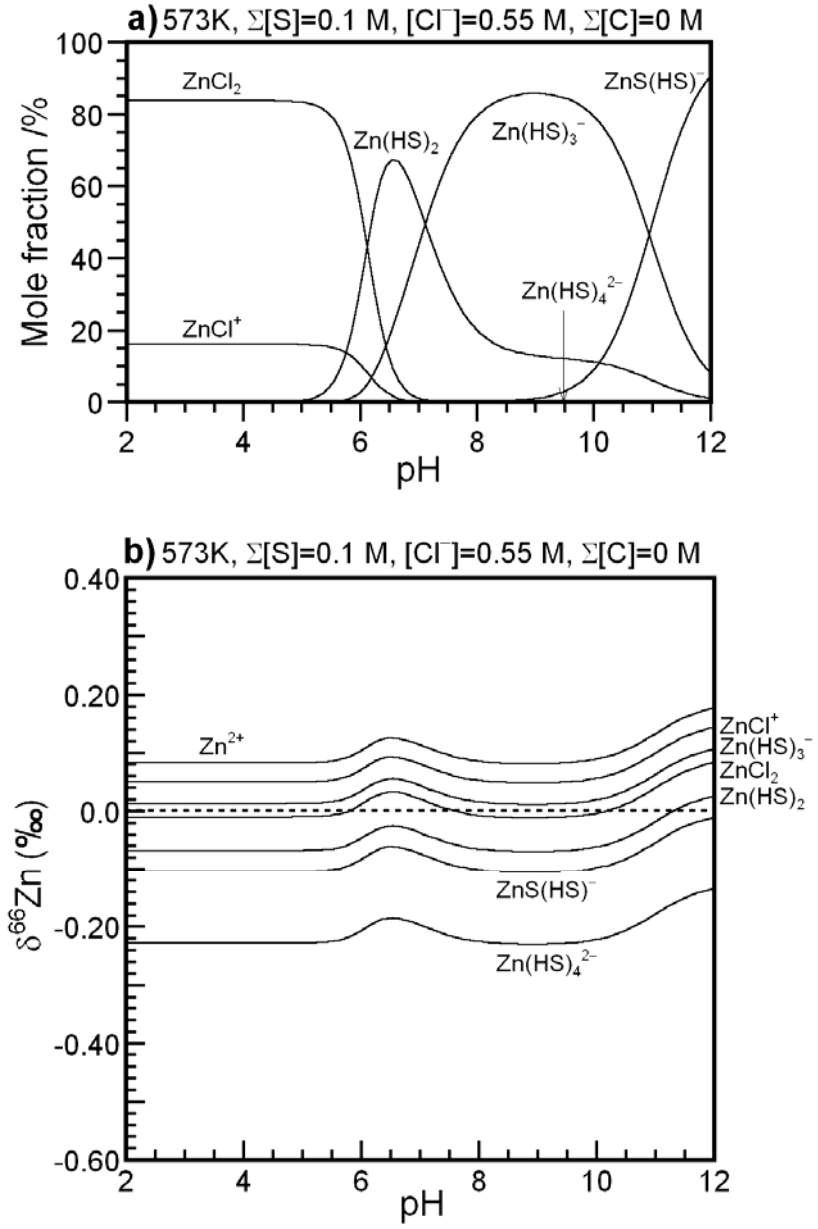

Fig. S5

Mole fractions of Zn species and Zn isotopic variations as functions of pH at 573 K (Σ[S] = 0.1 M, [Cl^-] = 0.55 M, and Σ[C] = 0 M). a) Mole fractions of Zn species in carbonate free hydrous fluid under Σ[S]=0.1 M and [Cl^-] = 0.55 M, b) δ^{66}Zn in carbonate free hydrous fluid. Mole fraction of Zn^{2+} is smaller than 0.001%. The maximum value of $Zn(HS)_4^{2-}$ mole fraction is 0.02% at pH=9.5. Dotted line in b) means δ^{66}Zn of bulk solution (averaged δ^{66}Zn in the whole solution). Σ[Zn] was set to be $10^{-6.1}$ M (Tagirov and Seward, 2010).

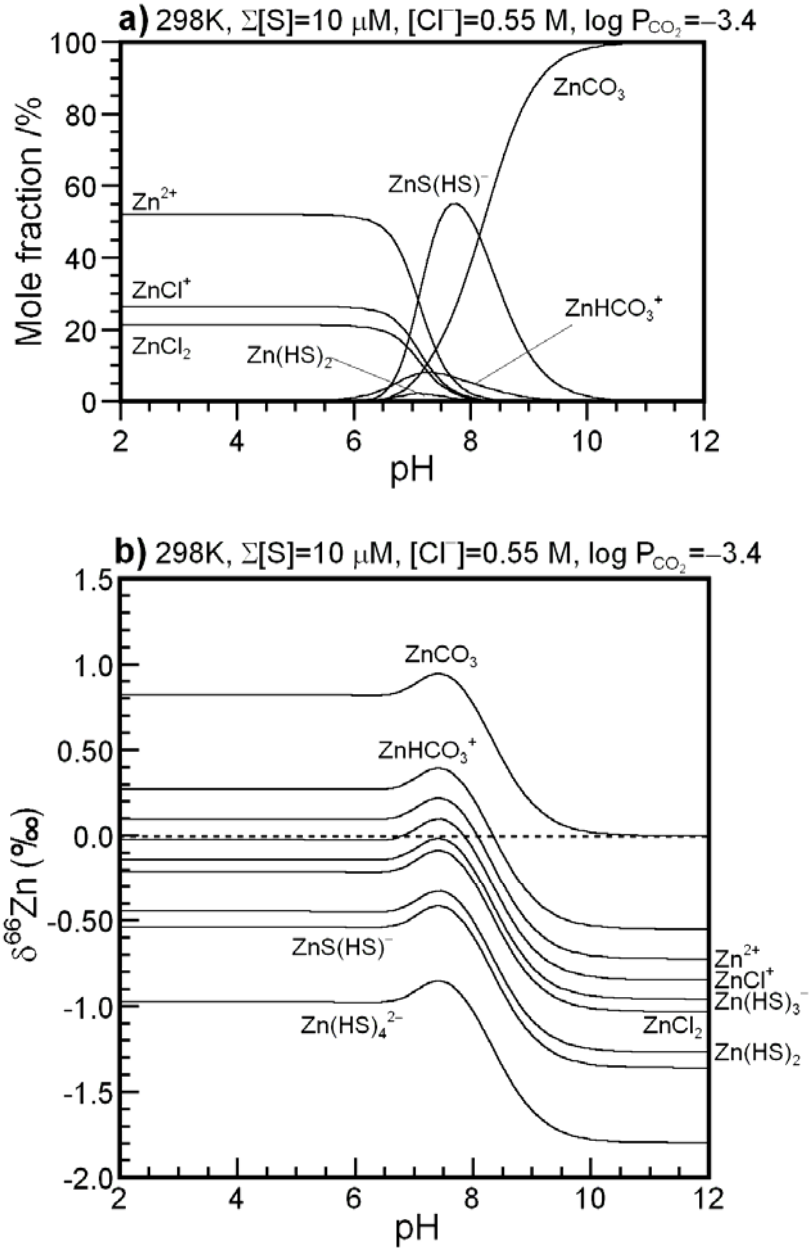

Fig. S6

Mole fractions of Zn species and Zn isotopic variations as functions of pH at 298 K (Σ[S] = 10 μM, [Cl^-] = 0.55 M, and log P_{CO2} = –3.4). a) Mole fractions of Zn species in hydrous fluid under low Σ[S] and P_{CO2} condition, b) δ^{66}Zn in the hydrous fluid. Σ[S] and P_{CO2} were set much smaller than those of Figs. 3a and 3c. The maximum value of $Zn(HS)_3^-$ mole fraction is 0.06% at pH=7.3. The maximum value of $Zn(HS)_4^{2-}$ mole fraction is 0.00001% at pH=7.4. Dotted line in b) means δ^{66}Zn of bulk solution (averaged δ^{66}Zn in the whole solution). Σ[Zn] was set to be $10^{-6.1}$ M (Tagirov and Seward, 2010).

References

Becke A. D. (1993) Density-functional thermochemistry. 3. The role of exact exchange. *J. Chem. Phys*. **98**, 5648-5652.

Black J. R., Kavner A., and Schauble E. A. (2011) Calculation of equilibrium stable isotope partition function ratios for aqueous zinc complexes and metallic zinc. *Geochim. Cosmochim Acta*, **75**, 769-783.

Frisch M. J., Trucks G. W., Schlegel H. B., Scuseria, G. E., Robb M. A., Cheeseman J. R., Montgomery Jr. J. A., Vreven T., Kudin K. N., Burant J. C., Millam J. M., Iyengar S. S., Tomasi J., Barone V., Mennucci B., Cossi M., Scalmani G., Rega N., Petersson G. A., Nakatsuji H., Hada M., Ehara M., Toyota K., Fukuda R., Hasegawa J., Ishida M., Nakajima T., Honda Y., Kitao O., Nakai H., Klene M., Li X., Knox J. E., Hratchian H. P., Cross J. B., Adamo C., Jaramillo J., Gomperts R., Stratmann R. E., Yazyev O., Austin A. J., Cammi R., Pomelli C., Ochterski J. W., Ayala P. Y., Morokuma K., Voth G. A., Salvado, P., Dannenberg J. J., Zakrzewski V. G., Dapprich S., Daniels A. D., Strain M. C., Farkas O., Malick D. K., Rabuck A. D., Raghavachari K., Foresman J. B., Ortiz J. V., Cui Q., Baboul A. G., Clifford S., Cioslowski J., Stefanov B. B., Liu G., Liashenko A., Piskorz P., Komaromi I., Martin R. L., Fox D. J., Keith T., Al-Laham M. A., Peng C. Y., Nanayakkara A., Challacombe M., Gill P. M. W., Johnson B., Chen W., Wong M. W., Gonzalez C., and Pople J. A. (2003) *Gaussian 03, Revision B.05*, Gaussian, Inc.: Pittsburgh PA.

Hay P. J. and Wadt W. R. (1985a) Ab initio effective corepotentials for molecular calculations. Potentials for potassium to gold including the outermost core orbitals. *J. Chem. Phys*. **82**, 299–310.

Hay P. J. and Wadt W. R. (1985b) Ab initio effective core potentials for molecular calculations. Potentials for the transition metal atoms scandium to mercury. *J. Chem. Phys.* **82**, 270–283.

Lee C. T., Yang W. T., and Parr R. G. (1988) Development of the colle-salvetti correlation-energy formula into a functional of the electron-density. *Phys. Rev. B* **37**, 785-789.

Tagirov B. R. and Seward T.M. (2010) Hydrosulfide/sulfide complexes of zinc to 250 °C and the thermodynamic properties of sphalerite. *Chem. Geol*. **269**, 301–311.

Wadt W. R. and Hay P. J. (1985) Ab initio effective core potentials for molecular calculations. Potentials for main group elements sodium to bismuth. *J. Chem. Phys.* **82**, 284–298.